Archaeological and Anthropological Sciences (2025) 17:88
https://doi.org/10.1007/s12520-025-02199-2

RESEARCH

Quantifying Levallois: a 3D geometric morphometric approach to Nubian technology

Emily Hallinan[1] · **João Cascalheira**[1]

Received: 15 October 2024 / Accepted: 27 February 2025 / Published online: 24 March 2025

Abstract

Levallois technology, a hallmark of Middle Palaeolithic stone tool manufacture, involves sophisticated core reduction strategies that have major implications for understanding human cognitive and technological evolution. However, traditional methods of analysing Levallois cores often fail to capture the nuanced variability in their morphology. This study introduces a novel application of three-dimensional geometric morphometrics (GM) to quantify the shape variability of Nubian Levallois cores from the Nile Valley and Dhofar regions. By employing this technique, we analysed core surfaces and preferential scar shapes, identifying distinct regional and technological patterns. Our results reveal significant inter-regional differences in core elongation and surface convexity, highlighting the importance of shape-oriented, rather than metric-based, analysis of prepared cores. This new GM approach offers a robust and replicable tool for investigating lithic variability and holds potential for broader applications in Palaeolithic research, enhancing our understanding of human technological adaptations.

Keywords 3D geometric morphometrics · Levallois · Lithic technology · Nubian Levallois cores

Introduction

Levallois technology is regarded as a hallmark of stone tool manufacture in the Middle Stone Age in Africa and the Middle Palaeolithic of Europe and western Asia, associated with at least three hominin species – early humans, anatomically modern humans and Neanderthals (Foley and Lahr 1997; Tryon et al. 2005; Hublin 2009). Named after the area in France, Levallois-Perret, where it was first described (Boucher de Perthes 1857; de Mortillet 1883; Commont 1909), Levallois is a type of prepared core technology that involves preparation of the convexities of the core surface and faceting of the striking platform to control the shape and size of the final end-product. The degree of planning involved in the pretermination of the Levallois end-product has been viewed as an indicator of cognitive complexity owing to the conceptualisation of the final core and product form, the sequential method required to achieve it, and social learning to transmit the process (Schlanger 1996; Lahr and Foley 2001; Wynn and Coolidge 2004; Lycett et al. 2016). The implications of Levallois for technical and economic behaviour has also seen varied interpretations, related to its efficiency (Brantingham and Kuhn 2001; Sandgathe 2004; Lycett and Eren 2013) and the role of its end-products (Sisk and Shea 2009; Eren and Lycett 2016; Shimelmitz and Kuhn 2018). Despite the central place that Levallois occupies in human evolution, its definition (Copeland 1983; Van Peer 1992; Dibble and Bar-Yosef 1995) and identification of both the technology (Hu et al. 2019a, 2019b; Li et al. 2019; Pallo 2022) and specific Levallois methods in assemblages (Rose et al. 2011; Goder-Goldberger et al. 2016; Blinkhorn et al. 2021a, 2021b; Hallinan et al. 2022a) remain highly debated topics.

Definitions of Levallois have shifted over the past decades, yet shape remains a key concept in all of them. In an early typological approach, Bordes (1950, 1961, 1980) emphasised that the predetermined shape of the Levallois flake was achieved through special preparation of the core prior to its removal, whereby different configurations of preparatory flaking generated end-products with different morphologies – flakes, blades or points. Accordingly, the morphology of the Levallois core was strongly tied to the end-product shape: an oval core produced an oval flake, a triangular core produced a triangular flake. Subsequent technological approaches shifted attention away from the final

✉ Emily Hallinan
Eshallinan@ualg.pt

[1] Interdisciplinary Center for Archaeology and Evolution of Human Behaviour, University of Algarve, Faro, Portugal

flake form towards understanding the Levallois reduction process (Bar-Yosef and Dibble 1995). Boëda's (1988, 1994, 1995) widely applied Levallois concept focuses on the geometric structure of the core as a volume, worked through a series of steps and fulfilling certain criteria. The volume of the Levallois core must consist of two asymmetric convex hemispheres that possess a plane of intersection at the core's margin. These hemispheres or surfaces are hierarchically related, each serving a specific, fixed role in reduction: a preparation surface for the production of striking platforms, and a flaking surface for the removal of the Levallois product. The flaking surface possesses both lateral and distal convexities that must be maintained to control the direction of force for the end-product, which is removed parallel to the plane of intersection. Viewed within a technological framework, it is the pattern and orientation of the preparatory flaking – not the core shape itself – that determines the morphology of the end-product (Boëda 1995; Van Peer 1992). However, whether lithic analyses are conducted from a typological or technological perspective, they encounter the same limitations – that shape is a qualitative, rather than quantitative variable.

Geometric morphometrics and Levallois morphology

Geometric morphometric (GM) approaches provide a statistical framework for studying shape variation – where shape is the specific geometric configuration of a specimen – independently of size (Slice 2007). Originally developed for applications in biological sciences (Rohlf and Marcus 1993; Adams et al. 2004), GM has gained traction as a powerful tool for quantitative analysis of shape across different aspects of lithic studies, though most commonly applied to bifaces, flakes and points since these can be consistently orientated and aligned according to geometrically correspondent points (e.g. Lycett et al. 2006; Archer and Braun 2010; Iovita 2011; Archer et al. 2016, 2018; Herzlinger et al. 2017; Herzlinger and Grosman 2018; Archer and Presnyakova 2019; Okumura and Araujo 2019; Timbrell et al. 2022a). As a consequence, most current GM studies that relate to Levallois technology have focused on debitage, using two-dimensional (Eren and Lycett 2012; Picin et al. 2014; Buchanan et al. 2023) and, occasionally, three-dimensional techniques (Chaćon et al. 2016; González-Molina et al. 2020; Delpiano et al. 2021; Bustos-Perez et al. 2024). The problem of identifying homologous points between specimens for comparison has meant that the application of GM to cores has been limited, since this artefact type displays marked variability in form through continuous, non-uniform reduction trajectories. However, the highly structured geometry of Levallois cores means that common features can be identified between specimens and therefore shape can be compared objectively (Lycett et al. 2010; Lycett and von Cramon-Taubadel 2013).

Prior application of 3D GM to shape variability in Levallois cores compared centripetal preferential Levallois specimens from Africa and Eurasia (Lycett and von Cramon-Taubadel 2013). This found relatively limited differences between core samples across space and time, with outline (planform) shape showing the greatest variability, whereas the least variation was seen in the topology of the upper flaking surface. This is consistent with the Levallois concept which concerns controlling the convexity of the upper surface. Critically, this also implies that outline shape of Levallois cores is the attribute most likely to reflect regionally or temporally distinct traditions, with Nubian Levallois cited as one possible example of this (Lycett and von Cramon-Taubadel 2013). Nubian Levallois technology was also central to an earlier study of the factors affecting Levallois end-product shape in Van Peer's (1992) analysis of Nile Valley Middle Palaeolithic assemblages. Through attribute analysis and refitting, Van Peer demonstrated that, rather than core shape, the organisation of scar ridges on the Levallois surface is key in guiding the preferential removal and thus are what dictate the end-product shape. In Nubian cores, the steep angle of this guiding distal median ridge (DMR) is regarded as a characteristic feature of Nubian core morphology (Usik et al. 2013).

Nubian Levallois describes a specific method for producing pointed end-products, named after the Nubian region of present-day southern Egypt and northern Sudan where it was first defined (Guichard and Guichard 1965; Hallinan and Marks 2023). Recently, the strict definition of Nubian Levallois cores has become important for identifying cores in regions beyond Nubia, with implications for the distribution of Nubian technology in terms of human demographic and cultural behaviour (Usik et al. 2013; Hallinan et al. 2022b). Shape is an important variable in a number of the defining attributes of Nubian technology and its end-products, but currently this is recorded descriptively (e.g. triangular, cordiform, pitched; Usik et al. 2013), or characterised using indices of elongation (length to width ratio), and flattening (width to thickness) (e.g. Blinkhorn et al. 2021a; Samawi and Hallinan 2024). However, this does not adequately capture shape either in two-dimensional outline or three-dimensional volume, and therefore important aspects of Nubian Levallois morphology and variability remain unexplored.

This paper presents a new approach for using 3D digital techniques to characterise the attributes that define Nubian Levallois cores, addressing morphological variability within and between Nubian core assemblages. In this proof-of-concept study, we apply our method to 3D analysis of Middle Palaeolithic assemblages from sites with Nubian Levallois cores from two regions: the Nile Valley in Egypt, and Dhofar in southern Oman. Using the analytical tools of a GM

approach, we test a series of hypotheses arising out of prior work on shape in Levallois technology:

Shape and size relationship: Differences in Levallois core shape will be independent of size, because shape is maintained throughout the knapping process (Boëda 1995, 2013).
Core and end-product shape covariation: The morphology of the core is related to the morphology of the end-product (Bordes 1980).
Technological variability: The organisation of scar ridges (i.e. core preparation strategy) determines end-product shape (Van Peer 1992).
Regional variability: Core outline shape, as opposed to topology of the two surfaces, is most likely to reflect regionally distinct traditions (Lycett and von Cramon-Taubadel 2013).

Materials and methods

Materials

The lithic samples derive from the Nile Valley sites of Nazlet Khater 1 (Middle and Upper levels) and Nazlet Khater 3 (NK), and two unpublished Dhofar surface artefact collections (TH). These assemblages contain Nubian Levallois cores whose technological characterisation is not disputed, meeting the generally-accepted criteria for this artefact type (Usik et al. 2013; Hallinan et al. 2022b). Nubian reduction is characterised by three main strategies of preparation to create the central ridge that guides the preferential removal. This can be achieved through distal removals (elsewhere described as 'Type 1 Nubian' (Guichard and Guichard 1965)), lateral removals ('Type 2'), and a combination of both distal and lateral removals ('Type 1/2' (Olszewski et al. 2010; Usik et al. 2013)). The analysed samples in this study include only complete cores which preserve a preferential scar outline and a clear DMR (Tables S1-S2). Levallois end-products from NK were included for comparison with the scar outline. These possessed varied dorsal scar patterns, meaning that they could derive from both Nubian or 'Classical' Levallois cores (Van Peer 1992). Products in the analysed sample had a generally convergent distal end shape, although this encompassed products with wide-ranging morphologies (Table S3).

Nazlet Khater (NK)

The NK sites were identified during surveys on the west bank of the River Nile in 1976 as part of the Belgium Middle Egypt Prehistoric Project, with the lithic material currently curated at KU Leuven, Belgium (Vermeersch et al. 1977, 1979). The studied assemblages derive from buried – albeit undated – stratified contexts, at NK1 divided into Middle (NK1-M) and Upper (NK1-U) assemblages. The underlying Lower assemblage was excluded from this analysis owing to the small sample size, and although the Upper layer was initially divided into A and B horizons, these were later deemed to be homogenous by the excavators (Vermeersch et al. 2002a). Both NK1 and NK3 were interpreted as chert quarrying sites owing to the availability of high-quality chert cobbles in nearby Nile and wadi deposits (Vermeersch et al. 2002a, 2002b).

The Nubian Levallois reduction method occurs alongside 'Classical' centripetally-prepared Levallois flake production. While Nubian cores substantially outnumber 'Classical' cores (the latter comprising 25% and 18% of the Levallois cores in the Middle and Upper assemblages respectively), these proportions do not correspond with Levallois end-products attributed to each method based on dorsal scar patterns ('Classical': NK1-M 55%; NK1-U 49%) (Vermeersch et al. 2002a, 2002b). This raises two questions; firstly, whether end-products can be reliably distinguished from different Levallois reduction methods, and secondly, whether during a full reduction sequence the two methods could be applied to the same cores. Van Peer (1992) rejects this latter scenario of flexible implementation of different Levallois methods since it is unsupported by the refit sequences. However, in a brief reassessment of 35 'non-Nubian' Levallois cores from NK1-Upper (presumed to be categorised as Classical in previous analyses), numerous cores were observed to possess a remnant distal platform and muted distal median ridge, suggesting there may be some more nuanced aspects to Levallois reduction at the sites. The 115 Nubian cores included in the sample show a predominantly distal preparation strategy (75.7%), with a small number of bilaterally prepared cores (6.1%), and in contrast to previous analyses of the assemblages, Nubian cores with both distal and lateral removals were also distinguished (16.5%) (Table S2).

Dhofar (TH)

The TH assemblages were collected in 2023 as part of the Czech ARDUQ Expedition to the Dhofar Nejd Plateau in southern Oman, where Nubian Levallois technology has been identified at hundreds of surface localities (Rose et al. 2011, 2023). Two new surface collections were made for the purposes of generating comparative samples for this study to test the analytical potential of the GM method. These were systematic but selective, including only complete and unambiguous Nubian Levallois cores. TH.571 derives from a desert pavement at the edge of a sedimentary basin, while the TH.584 artefacts were eroding from a buried pediment. Chronometric ages are pending from both deposits, but an OSL age of 106 ka has been obtained from sediments

containing a buried core at nearby site Aybut Al Auwal (TH.59), located approximately 250 m from TH.584 (Rose et al. 2011). Both assemblages are primary exploitation sites associated with large, tabular chert slabs outcropping nearby. Future studies will use systematic collections from prior work in Dhofar (e.g. Rose et al. 2011; Usik et al. 2013) to investigate regional variability within Levallois technology more comprehensively.

There are several key differences between the TH and NK assemblages: first, Nubian Levallois is the only Levallois core reduction strategy present in almost all Dhofar Middle Palaeolithic assemblages, and furthermore there are very few non-Levallois cores. Additionally, Levallois end-products are scarce at most sites which may reflect different patterns of landscape use between the Nile Valley and the Nejd plateau, as well as the types of site studied. The Dhofar Nubian cores also show more varied patterns of preparation than the predominantly distal preparation at NK, using mainly bilateral (41.2%) and a combination of distal and lateral (45.1%) removals (Table S2). It is worth noting that at several other Dhofar sites, distally-prepared cores are proportionally more common than in these two particular assemblages (Usik et al. 2013; Rose et al. 2018).

Methods

The specific features that define Nubian cores were captured on 3D models of artefacts using landmark and semilandmark (SLM) points, complemented by qualitative attribute data (Table 1). Landmark processing, GM and statistical analyses were carried out in R (R Core Team 2024) using functions in the packages Morpho (Schlager 2017) and geomorph (Baken et al. 2021; Adams et al. 2024). Full details are provided in the accompanying research compendium (https://doi.org/10.17605/OSF.IO/SJ8ZV), and supplementary figures and tables.

3D data acquisition

Artefacts were scanned by one of us (EH) using an Einscan Pro 2 × Plus structured light scanner. Each specimen was captured in multiple orientations to ensure complete coverage and these scans were automatically aligned in the associated Shining 3D software. Mesh models were also generated with this software at medium resolution, exported in PLY format, and simplified using the quadric edge decimation resampling tool in Meshlab (quality threshold 0.3).

Landmarking: Cores

Defining landmarks as homologous points that correspond between specimens is complex on archaeological artefacts and therefore these must be chosen carefully and consistently. Nubian cores possess more distinctive and standardised morphological features than some other Levallois core types, making them an ideal test-case. A new protocol for landmarking cores was adapted from the method used by Archer et al. (2018, 2021) for blanks, using the software Landmark V3 (University of California, Davis) for landmark placement with subsequent processing in R (R Core Team 2024). Technologically meaningful, homologous points were identified based on defining morphological features of Nubian cores: the opposed proximal (preferential) and distal (preparation) platforms. One landmark was placed at the distal extremity and two at the lateral extremities of the proximal platform. Three curves consisting of 20 semilandmarks (SLMs) each were placed around the core edge between these points, bisecting the upper and lower surfaces of the Levallois core (Fig. 1A). Seven SLMs were placed along the DMR in order to take digital angle measurements; however, they are excluded from the analysis presented here due to complicated measurement parameters (discussed further

Table 1 Characteristics defining Nubian Levallois cores (after Usik et al. 2013, updated in Hallinan et al. 2022b) and how these attributes were recorded

Criteria in Hallinan et al. 2022b	Attribute in Usik et al. 2013	In this paper
1. Steep distal ridge of 90 degrees or less	Numerical: 60–120 degrees	Semilandmarked surface patch captures the distal ridge morphology in 3D*
2. Distal (preparation) and proximal (preferential removal) platforms serving alternate roles	Qualitative	Landmarked points at the distal tip and extremes of the proximal platform
3. Distal and/or lateral preparation strategy	Qualitative: Nubian Types 1, 2 or 1/2	Qualitative: distal, left lateral and right lateral preparation (and combinations of these), and Nubian Types 1, 2 and 1/2
4. Convergent core morphology	Qualitative: triangular, pitched, cordiform	Semilandmarked outline at intersection of Levallois surfaces captures planform morphology
5. Production of pointed end-products	Qualitative	Semilandmarked outline of final/preferential scar negative

*Seven semilandmarks were also positioned along the distal ridge for digital angle measurement of the DMR; this is excluded from the analyses presented here

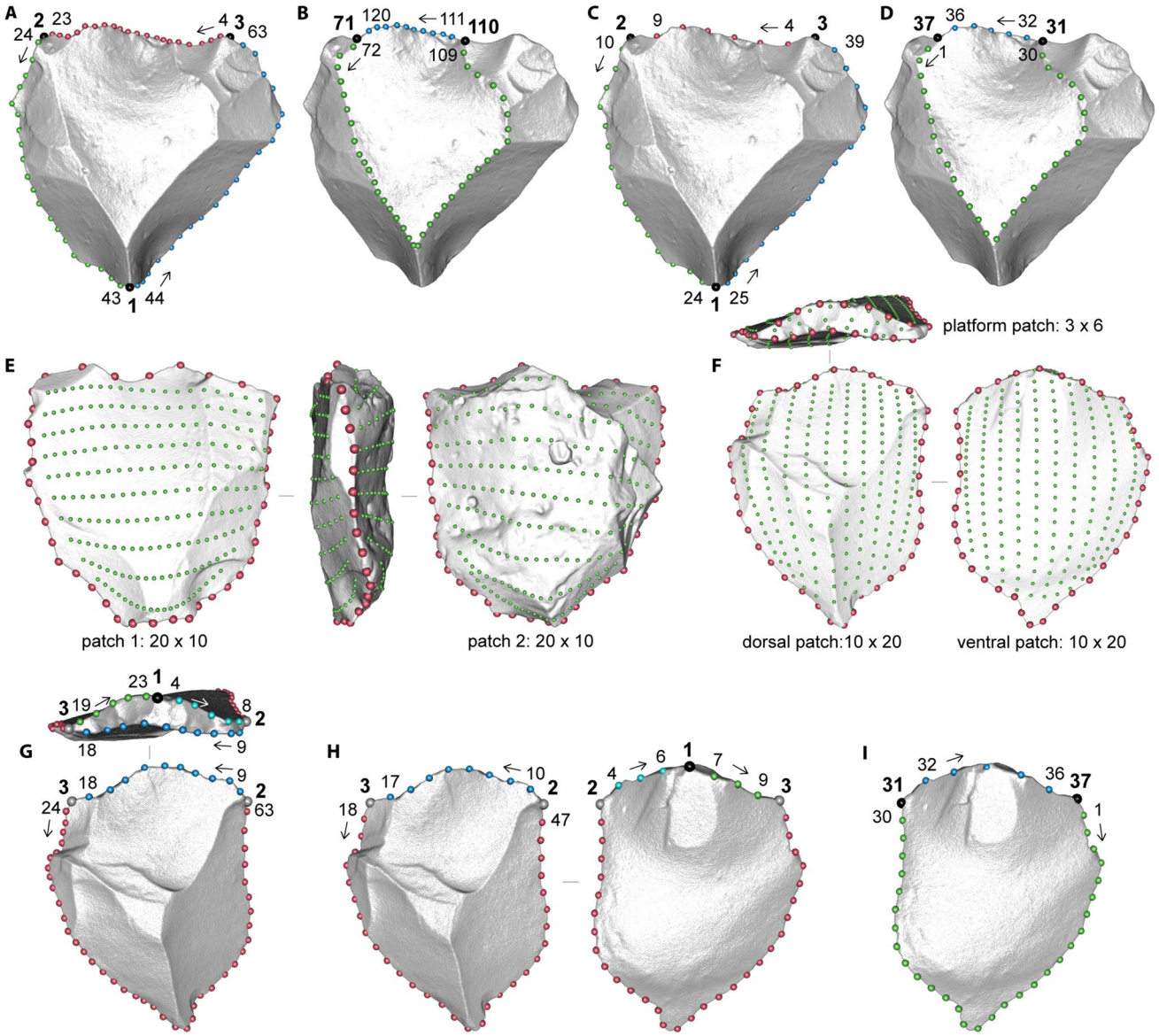

Fig. 1 Landmark configurations for cores and end-products during processing steps. **A** core outline landmarks after manual placement; **B** preferential scar landmarks after manual placement; **C** core outline semilandmarks after resampling and sliding; **D** preferential scar outline semilandmarks after resampling and sliding; **E** upper and lower surface patch placement on a template core; **F** platform, dorsal and ventral surface patch placement on a template product; **G** platform and outline landmarks after manual placement (different colours reflect curves); **H** product outline semilandmarks after resampling and sliding; **I** extracted ventral outline after resampling and sliding

below; Valletta et al. 2020; Yezzi-Woodley et al. 2021; Schunk et al. 2023; Muller et al. 2024). The preferential (or final) scar was outlined with 10 platform and 40 edge SLMs (Fig. 1B). Two surface patches were placed on the upper and lower core faces of one arbitrarily selected artefact to be used as a template for other specimens (Fig. 1E).

These co-ordinate configurations were imported into R with the platform points treated as fixed landmarks and the points around the core and preferential scar outline as sliding SLMs. Using functions in R, these were resampled as equally-spaced SLMs and then slid along the mesh model surface (Fig. 1C-D). The SLM configuration of the surface-patched specimen was deformed onto the other specimens to generate geometrically correspondent surface co-ordinates across all cores.

Landmarking: End-products (blanks)

The landmarking protocol followed by Archer et al. (2018, 2021) for blanks was replicated on Levallois end-products. Three fixed landmarks were placed on the platform (at the point of percussion and lateral extremities of the platform)

to allow uniform orientation of the artefacts. Four curves formed of SLMs between these points (three platform curves of 5, 5 and 10 SLMs, and one of 40 around the flake edge) served to capture the flake outline (Fig. 1G). Three surface patches were placed on the platform, dorsal and ventral faces of one arbitrarily selected template artefact (Fig. 1F). Following the same steps as for cores outlined above, edge curve SLMs were resampled and slid (Fig. 1H), and the surface-patched template was deformed across all of the other specimens. Lastly, the SLMs outlining the ventral face were extracted and resampled for shape comparison with core preferential scar outlines (Fig. 1I).

GM analyses

The processed landmark configurations were subjected to Procrustes superimposition, a process required for statistical shape analysis that removes differences related to size and orientation by scaling and aligning all specimens (Goodall 1991). Generalised Procrustes Analysis (GPA) superimposes landmark configurations using the mean shape as the target for comparison (Slice 2007; Adams and Otárola-Castillo 2013). Subsequent statistical analyses were carried out on the co-ordinates of these Procrustes-aligned shapes.

To assess allometry (i.e. whether size and shape vary independently), artefact shapes were regressed against their log-transformed centroid sizes using a generalised linear model (Klingenberg 2016). In GM, centroid size is a measure of overall size that treats size as mathematically independent of shape, therefore does not rely on the distance between any two points (Bookstein 1991). It is calculated as the square root of the sum of squared Euclidean distances of all landmarks from their centroid (the mean of all landmark coordinates; the centre of gravity). The regression slope of the (Type 1) linear model was compared against a null model of isometric change in a Procrustes ANOVA on the sum of squared Procrustes distances (Goodall 1991). In the null model, isometric change (size and shape are independent) has a slope of zero, and allometric change (size and shape are dependent) a non-zero slope. The significance of covariation of shape and size was tested using a non-parametric residual randomised permutation procedure with 1000 permutations, based on Goodall's F-statistic (Goodall 1991).

Principal Components Analysis (PCA) was performed on the covariance matrix of the aligned artefact shapes, with each component capturing aspects of variation in shape space. Outliers were identified as specimens with Procrustes distances exceeding three standard deviations of the mean shape and were excluded from the PCA (Table S1). PC plots of the components accounting for the greatest variability in the dataset allowed comparison of groups in the data (core surfaces, preferential scars and NK products), using attributes such as region and core preparation strategy. The minimum and maximum extremes of shape on each PC axis were visualised in relation to the mean landmark configuration in order to understand the nature of shape variation each component described. One-way ANOVAs using Type III sums of squares were conducted on individual PC scores to test for significant differences between groups. Further multivariate ANOVAs (MANOVA) were used to examine interactions between variables where relevant. To understand the specific differences between pairs of attributes, post-hoc Tukey's Honest Significant Difference (HSD) tests compared the means of each combination of categories.

To compare covariation between two sets of co-ordinates on the same specimen (core outline shape and preferential scar shape), a two-block partial least squares method (PLS) was used (Rohlf and Corti 2000). This relationship was visualised by plotting two-block PLS scores of core outlines against those of preferential scars on the first dimension (i.e. the maximum covariance) using a generalised linear model.

Results

Shape and size relationship

All prior comparative studies of Nubian Levallois cores have used core size as the primary quantitative basis for analysis (e.g. Hilbert et al. 2016; Groucutt & Rose 2023; Samawi and Hallinan 2024). Dimensions (length, width, thickness and their ratios) are the most commonly quantified attributes on lithic artefacts, yet these measurements not always replicable between researchers (Pargeter et al. 2023). Three-dimensional models offer an alternative to dimensional metrics, with centroid size used as the standard measure of size in GM analyses (Klingenberg 2016). Centroid size is calculated as the square root of the sum of squared distances from all landmarks to their centroid (the geometric centre; the average of all landmark x, y and z coordinates), providing a relative measure of overall geometric scale that is independent of shape. The relationship between Nubian core size and shape in the NK and TH samples was first examined using standard artefact dimensions, followed by GM methods to test whether centroid size was representative of traditional size measurements.

The mean length of TH cores is nearly twice that of NK cores (TH mean: 111 mm, NK mean: 60 mm), with even the smallest TH cores larger than the NK average (TH range: 68.2–174.5 mm) (Table S5). Although metric variability is limited between the three NK assemblages, TH.571 is markedly larger than TH.584, by a factor of 1.3 across all dimensions. Elongation (length/width) and flattening (width/thickness) indices indicate that TH cores are more elongated (1.4) than NK (1.2), while NK1 cores are flatter (2.6) than those at NK3 and the TH sites (2.4). Therefore, the principal

differences between regional assemblages are that TH cores are both substantially larger, and are more elongated, than NK cores. When centroid size is used as an overall indicator of core size, this upholds the same patterns as length, whereby the mean value for TH cores is also double that of NK (TH: 835, NK: 443) Fig. 2A, Table S6). These differences were found to be strongly statistically significant in a Welch's T-test ($T = 19.8$, $P < 0.001$). Similarly, there is limited variation in mean centroid size among the NK assemblages (NK1-M: 455, NK1-U: 436, NK3: 445), while TH.571 (892) is larger than TH.584 (684) by a factor of 1.3, as observed in the dimensional metrics. Using the coefficient of variation (CV, calculated as the ratio of the standard deviation to the mean, expressed as a percentage) to assess size standardisation (Eerkens and Bettinger 2001), all assemblages show very high standardisation; NK3 shows the lowest (21%), and TH.571 the highest (10%) (Table S6). Regional mean values indicate higher standardisation among Dhofar cores (16%) than the Nile Valley (17%), which is similar to observations of CV on length for other assemblages from Dhofar (16%) and the Nile Valley (22%) (Samawi and Hallinan 2024). The overall strong agreement with standard metric results demonstrates that centroid size can be a useful – replicable – substitute in place of taking standard dimensional measurements on specimens that are subject to 3D scanning and GM analysis.

The covariation of size and shape is evaluated in GM in terms of allometry (a dependent relationship), or isometry (an independent relationship) (Klingenberg 2016). Allometry was assessed for core surfaces (i.e. 3D shape) and preferential scar outline by regressing these shapes against the natural log of their centroid sizes using a generalised linear model (Fig. 2B-C). The regression for all shapes shows a positive correlation, with distinct regional clusters of NK and TH cores. A Procrustes ANOVA for the whole Nubian core sample (i.e. not separating samples regionally) shows statistically significant weak to moderate positive allometry across all shapes (core surfaces: $F = 11.00$, $P < 0.001$; core outlines: $F = 16.65$, $P < 0.001$), being strongest for preferential scars ($F = 33.26$, $P < 0.001$) (Table 2, Table S7). However, given the marked centroid size differences between TH and NK cores, separate Procrustes ANOVAs were carried out to test whether region was the driver behind (albeit weak) positive allometry. The results for core surfaces show much lower F-statistic values, with weaker statistical significance (NK: $F = 2.14$, $P < 0.05$; TH: $F = 1.60$, $P < 0.1$), indicating that centroid size is a limited explanatory factor for intra-regional shape variation in Nubian cores (NK: 1.9% of variation; TH: 3.2%) (Table 2). Similarly low, though statistically significant, F-values were observed for preferential scars on cores (Table 2), favouring the null hypothesis that Nubian core shape variation is independent of differences in size in each region. Overall, when regional differences are removed, size is not a significant factor in determining Nubian core shape variation. This is consistent with a Levallois strategy that focuses on preparing a core surface to produce an end-product of a specific shape. Furthermore, it suggests that there may be other behavioural factors related to raw material, environment, function or culture that explain inter-regional core size differences (Samawi and Hallinan 2024).

Principal components analysis of shape variability

A PCA was conducted to explore aspects of Nubian core shape variation independent of size. The different principal components (PC) capture both the nature and percentage of total shape variance, showing that for all core surfaces, PC1 explains 19.7% of variance, followed by PC2 (14.9%) and PC3 (11.2%), with 66% of variance accounted for by the first six PCs (Table S8). PC1 mainly explains elongation, with high values indicating short, wide cores, while low values correspond to long, narrow cores (Fig. 3). High PC1 values also indicate a steep distal ridge angle, whereas this angle is shallow for low values. PC2 is driven by lateral skew, relating to the orientation of the distal tip and lateral twist in the profile of the plane of intersection (Fig. 3). PC3 relates to core profile and the distribution of mass between the two flaking surfaces (Fig. 4). Cores with high PC3 scores have greater volume concentrated in their upper surface, whereas the lower surface volume is greater for low scores. Additionally, cores with high PC3 values possess a steeper distal ridge, though this may partly be explained by the increased convexity of the upper face. Likewise, low PC3 scores correspond to a shallower distal convexity. PC4 describes the pointedness of the distal end of the core; low scores indicate a triangular shape, while high scores are more ovate with a rounded distal (Fig. 4). PCs 5 and 6 account for only 6–7% of the variance each but capture important differences in core thickness and convexity. High PC5 scores reflect thicker cores with pronounced surface convexities and a steep distal ridge, with low scores indicating flatter surfaces and a muted distal ridge angle (Fig. S1C). PC6 captures core thickness, particularly in the volume of the lower surface. Cores with low PC6 scores are flat with limited lower surface volume, while cores with high scores are thick with a large lower surface volume (Fig. S1C).

Regional variability

ANOVAs and appropriate post-hoc tests were performed on the key variables associated with the specimens: region, assemblage, preparation strategy and Nubian core type (Table 3, Table S9). High F-statistics indicate more variability between, than within, groups. The strongest shape differences are seen inter-regionally between the Nile Valley

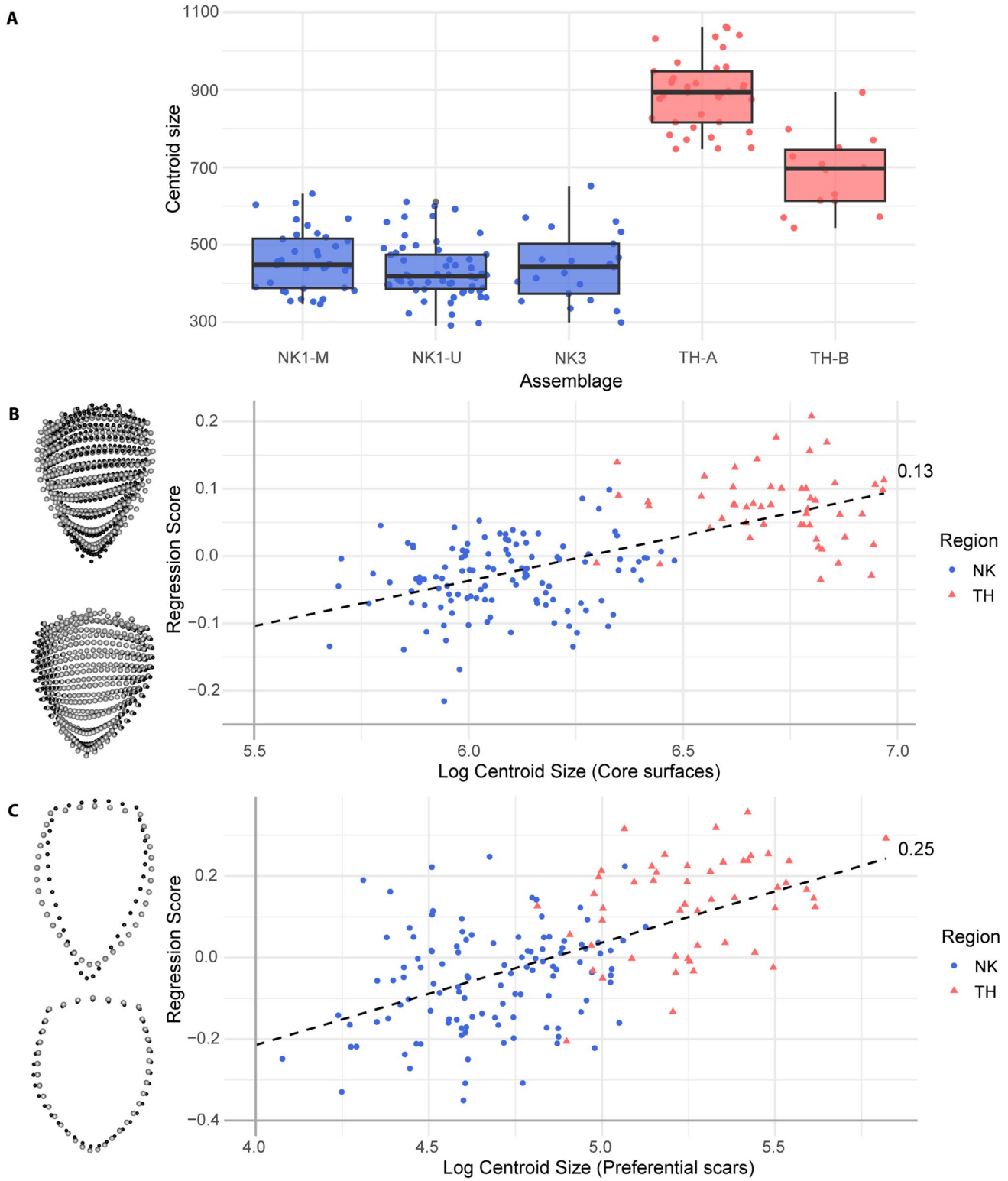

Fig. 2 Boxplot and linear regression plots of centroid size. **A** Boxplot of centroid size by assemblage; **B-C** Linear regression plot comparing shape changes (regression scores) against the natural logarithm of centroid size for core surfaces (**B**) and (**C**) preferential scar outline. The shapes representing minimum and maximum regression scores (black spheres), in relation to the mean shape (grey spheres) are shown adjacent to the y-axis

Table 2 ANOVA results for regressions of core and preferential scar shapes on the natural logarithms of centroid sizes (full results in Table S7)

Model	DF	R^2	F	Z	P
All core surfaces	1, 164	0.061	10.633	5.632	0.001 ***
All core outlines	1, 164	0.092	16.650	6.017	0.001 ***
All preferential scars	1, 164	0.169	33.257	5.051	0.001 ***
NK core surfaces	1, 113	0.019	2.143	1.928	0.024 *
TH core surfaces	1, 49	0.032	1.601	1.492	0.073 .
NK preferential scars	1, 113	0.033	3.881	2.431	0.006 **
TH preferential scars	1, 49	0.078	4.140	2.281	0.005 **

DF Degrees of freedom; R^2 Coefficient of determination; *F* Goodall's F-statistic; *Z* Effect size; *P* Significance levels: $P<0.001$ (***), $P<0.01$ (**), $P<0.05$ (*), $P<0.1$ (.)

(NK) and Dhofar (TH), particularly on PC1 (F = 44.97) and PC3 (F = 39.84, $P<0.001$), with moderate strength on PC2 (F = 8.33) and PC4 (F = 9.29, $P<0.005$), and weak on PC5 (F = 6.20) and PC6 (F = 5.80, $P<0.01$). TH cores have generally lower PC1 scores and are therefore more elongated than NK, thus supporting the elongation index based on length-to-width ratios (Table S5). TH cores tend to have higher PC3 values, indicating greater upper-surface convexity and correspondingly steep distal ridges. This difference is also expressed in higher PC5 and lower PC6 scores for TH cores, reflecting thick cores with a convex upper surface volume and a flatter lower surface. In contrast, NK cores have a more typical Levallois core morphology, with a flatter upper surface and convex lower surface. Both NK and TH encompass a similar range of variability on PC4, describing distal shape, although the highest-scoring specimens (ovate) are from the Nile Valley, and the lowest score (most pointed) is from Dhofar. It is likely that both extremes represent advanced stages of reduction.

At an assemblage level, strongest differences are expressed on PC1 (F = 13.52) and PC3 (F = 12.17, $P<0.001$), with high significance still observed on PC2 (F = 5.23) and PC6 (F = 5.06, $P<0.001$) (Fig. S1). Most of this variation is explained by regional differences, but NK3 presents an interesting case. The core sample from NK3 lies in between the other NK and TH sites on PCs 1 to 4, showing no statistically significant differences (Fig. S1A-B, Table S10); however, on PC6, NK3 significantly differs from NK1-M ($P<0.05$), TH.571 ($P<0.05$) and TH.584 ($P<0.001$) (Table S10). NK3 cores concentrate at the higher end of the spectrum (Fig. S1C), indicating greater lower surface volume and convexity. Based on dimensions alone, NK3 has similar mean values to the NK1 assemblages, but shows slightly higher elongation and lower flattening (Table S5). The volumetric concept underpinning Levallois cores emphasises the role of two asymmetric volumes (Boëda 1995), but this is difficult to capture quantitatively using standard metrics (Ranhorn et al. 2019). Thus, the insights offered here by comparing these aspects of shape reveal some nuanced differences between NK assemblages, as well as clear inter-regional distinctions between the Nile Valley and Dhofar (Fig. S2A-B).

Technological variability

Core preparation strategy (using Nubian core type as a simplified indicator of scar pattern) was considered to test whether technological, rather than regional, factors drive shape variation. The strongest differences are observed on PC3 (F = 14.01) and PC4 (F = 7.62, $P<0.001$), with a low F-statistic but still high significance on PC1 (F = 5.44, $P<0.005$) (Table 3, Fig. S3). Post-hoc tests identify that these differences are between Type 1 (distal preparation) and Type 2 (bilateral) cores on PCs 3 and 4, and between Type 1 and Type 1/2 (distal and bilateral) cores on PC3 (Table S10). Shape variation on PC3 corresponds to the relative volume and convexity of the core surfaces, therefore Type 1 cores have a shallow upper surface convexity, whereas this convexity is steep on Type 2 cores. PC4 relates to the distal shape of the core, indicating that Type 2 cores are generally more pointed than Type 1.

There are regional differences in the principal core preparation strategy used; Type 1 dominates at NK (76% of cores), whereas TH has high proportions of both Type 2 (41%) and Type 1/2 (46%). Therefore, a MANOVA was carried out for PC3 (showing the strongest relationship) to test for interaction between region and core type. This yielded significant results, with a low F-statistic of 7.06 (Table S11), meaning that while different core types have distinct shapes on PC3 (i.e. surface convexity), these may also vary according to region. The addition of Nubian core samples from further assemblages and regions will contribute to testing the strength of regional differences in future analyses.

Preferential scar shape variability

The shape of the Levallois end-product was represented by the preferential (or final) scar outline on the cores. PC1 captures 52.1% of variance, with moderate contributions from PC2 (16.6%) and PC3 (11.5%) (Table S12). PC1 represents the elongation of the scar, reflecting contrasting long, narrow (low scores) and short, wide (high scores) shapes (Fig. 5). PC2 captures asymmetry in terms of left or right skew of the product distal. PC3 corresponds to whether the distal shape is convergent (high scores) or divergent (low scores), reflecting pointed or ovate shapes.

Scar shapes show strong regional differences, particularly on PC1 (F = 64.52) and PC3 (F = 22.96, $P<0.001$) whereby products from TH cores tended to have higher PC3 and lower PC1 scores, representing very narrow pointed

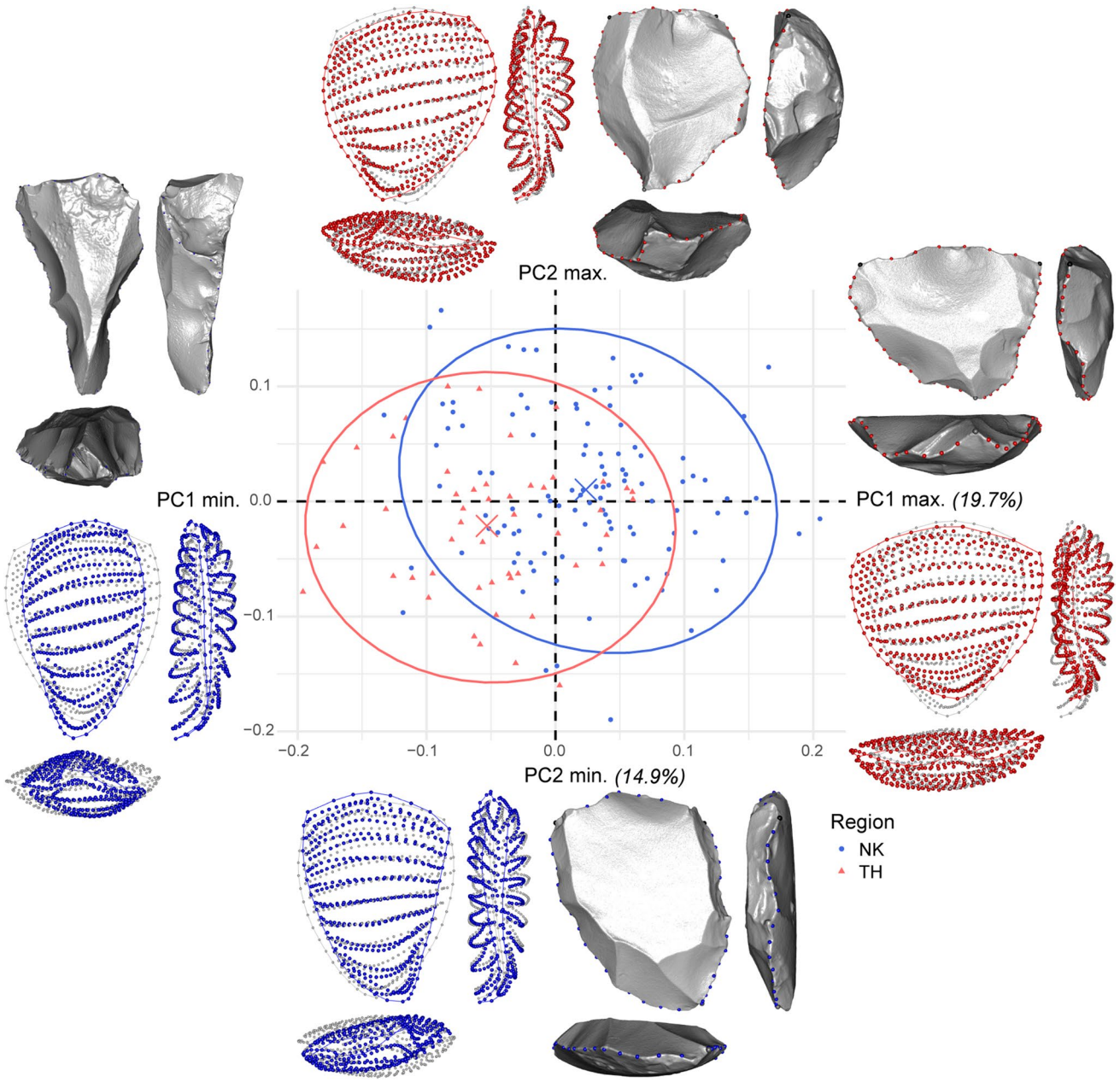

Fig. 3 PCA plot of principal components 1 and 2 for core surfaces, grouped by region. The mean PC score for each group is indicated by a cross (X). Mean (grey), minimum (blue), and maximum (red) theoretical shapes are depicted alongside actual minimum and maximum specimen shapes

shapes (Fig. 5, Table 3, Table S13). NK scars showed the inverse, reflecting products with short and wide shapes that might be better classified as flakes than points Fig. S2(C-E). There were also statistically significant differences at an inter-assemblage scale (PC1: $F = 17.39$; PC3: $F = 7.89$, $P < 0.001$), although this is most strongly expressed as regional differences between Nile Valley and Dhofar assemblages (Table 3). However, some finer-grained patterns suggest that NK3 scar shapes are more similar to TH.584 than the other NK assemblages (Table S14). This reinforces the observations for overall core shape, indicating that NK3 shares more similarities with TH assemblages than the other NK1 assemblages do.

Significant differences in scar shape are also present between cores of different Nubian types. As observed for core surface shape, on PC1, Type 1 core scars are significantly different from Type 2 and Type 1/2, with a post-hoc test indicating that the Type 1/2 scar pattern with the greatest (albeit weak) difference is distal-bilateral ($P < 0.1$) (Table S14). A MANOVA was also carried

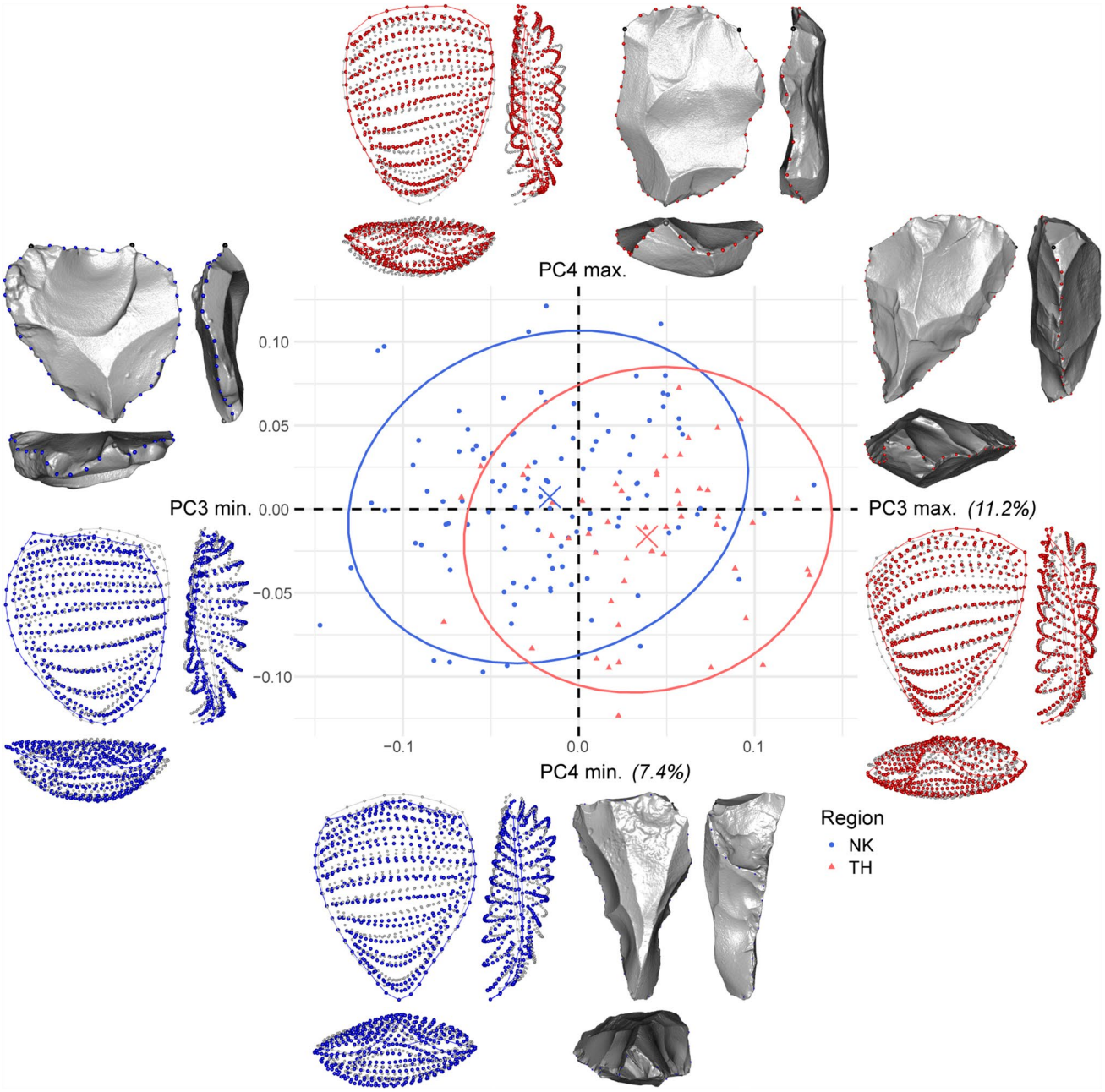

Fig. 4 PCA plot of principal components 3 and 4 for core surfaces, grouped by region. The mean PC score for each group is indicated by a cross (X). Mean (grey), minimum (blue), and maximum (red) theoretical shapes are depicted alongside actual minimum and maximum specimen shapes

out for scar shape on PC1, but no significant interaction between region and scar type was detected (Table S15). This means that in terms of the elongation of preferential scar, the shape differences observed between regions and Nubian type are independent of each other.

End-product shape variability

The shape (and size) of the final removal from a Levallois core will be sensitive to the stage and extent of core reduction, often encountering knapping accidents as the core

Table 3 ANOVA results for core and preferential scar shape for significant variables for the first 6 PCs (full results in Tables S9 and S13)

Shape	PC	% var	Region F	Region P	Type F	Type P	Assem F	Assem P	Prep F	Prep P
Core surface	PC1	19.7	44.971	0.000 ***	5.445	0.005 **	13.418	0.000 ***	2.650	0.018 *
Core surface	PC2	14.9	8.325	0.004 **	–	-	5.225	0.001 ***	–	–
Core surface	PC3	11.2	39.838	0.000 ***	14.011	0.000 ***	12.170	0.000 ***	5.320	0.000 ***
Core surface	PC4	7.4	9.294	0.003 **	7.618	0.001 ***	3.201	0.015 *	2.907	0.010 *
Core surface	PC5	7.0	6.200	0.014 *	–	–	–	–	–	–
Core surface	PC6	5.9	5.799	0.017 *	–	–	5.059	0.001 ***	–	–
Pref. scar outline	PC1	52.1	64.528	0.000 ***	14.796	0.000 ***	17.390	0.000 ***	5.580	0.000 ***
Pref. scar outline	PC3	11.5	22.962	0.000 ***	2.564	0.080 .	7.885	0.000 ***		

DF Degrees of freedom; *F* Goodall's F-statistic; *P* Significance levels: $P < 0.001$ (***), $P < 0.01$ (**), $P < 0.05$ (*), $P < 0.1$ (.)

is exhausted (e.g. step or hinge terminations). This places potential limitations on how indicative the scar shape is of products removed earlier in the core reduction. The NK assemblages contain substantial numbers of Levallois end-products, providing the opportunity to test for significant differences between last scar and product shape.

Considering first the 3D shape of product surfaces, PC1 explains 43.7% of variance, with moderate contributions from PC2 (15.0%) and PC3 (11.0%) (Table S16). PC1 represents product elongation, with low values reflecting long and narrow shapes and high values indicating short and wide shapes (Figs. 6 and S2F). PC2 captures asymmetry in terms of left or right skew of the product distal tip. PC3 corresponds to the convergence of the laterals, with low scores reflecting triangular shapes, while high scores have a circular shape. PC4 describes whether the greatest width of the product is at the proximal (low) or the distal (high) end. The only statistically significant shape differences between assemblages is on PC3, where NK1-U differs from both NK1-M and NK3 (Tables S17-S18). This contrasts with earlier results on cores that instead separate NK3 from the other NK assemblages, which may indicate biases either in the shapes of products taken away from the site, or in the product sample used for analysis.

A direct comparison of preferential scar and product outline shape shows significant differences on PC1 (49.5% of variance) and PC3 (10.7%) (Table S19, Fig. S4). Differences between scar and product shape are significant in terms of artefact type only on PC1, relating to elongation (Tables S20-S21). Significant inter-assemblage differences are expressed on PC3, describing the distal shape of the Levallois product removal (Tables S20-S21). This limited difference in shape suggests that core preferential scars sufficiently represent product shape variability, making this a useful proxy for studying assemblages where Levallois products are scarce, as is the case for many Nubian core assemblages (Chiotti et al. 2009; Usik et al. 2013).

Shape covariation and standardisation

To test the hypothesis of shape covariance – based on the principle that Levallois reduction aims to produce a product of a predetermined shape (Bordes 1980; Boëda 1995) – core outline and preferential scar shape were compared using a two-block PLS analysis. For the entire core dataset, this indicated a strong, statistically significant positive correlation between core outline and preferential scar shape (r-PLS = 0.63, $p < 0.001$), with 87% of covariance explained on the first dimension (Table 4). The test was then carried out for each regional sample separately to examine intra-regional patterning. For NK, a moderate correlation is observed (r-PLS = 0.46, $p < 0.001$), explaining 58% of covariance. In contrast, TH showed higher shape correlation, accounting for 57% of covariance, but this was not statistically significant (r-PLS = 0.56, $p = 0.1$), which could indicate more variability in shapes, or less distinct covariation compared to NK cores. Additional comparisons with other Dhofar assemblages could clarify this pattern regionally. For Nubian core types, moderate to strong correlations were found, with the highest significance for Type 1 cores (Table 4).

Linear regression analysis of scores for Block 1 (core outline as the predictor variable) and Block 2 (scar outline as the response variable) demonstrated that the model explained 40% of the variance for the entire core sample (Table 4, Fig. 7). Separate regression analyses were also conducted on regions and core types, finding a weak linear relationship for NK cores ($R^2 = 0.21$), indicating a less predictable correlation between core and scar shape. TH cores showed a stronger relationship ($R^2 = 0.31$), which suggests there is less variability compared to NK. Type 2 cores displayed the strongest model fit ($R^2 = 0.52$), indicating a more robust and predictable relationship between core and scar shape than for Type 1 ($R^2 = 0.27$) or Type 1/2 cores ($R^2 = 0.35$). Overall, while the two-block PLS

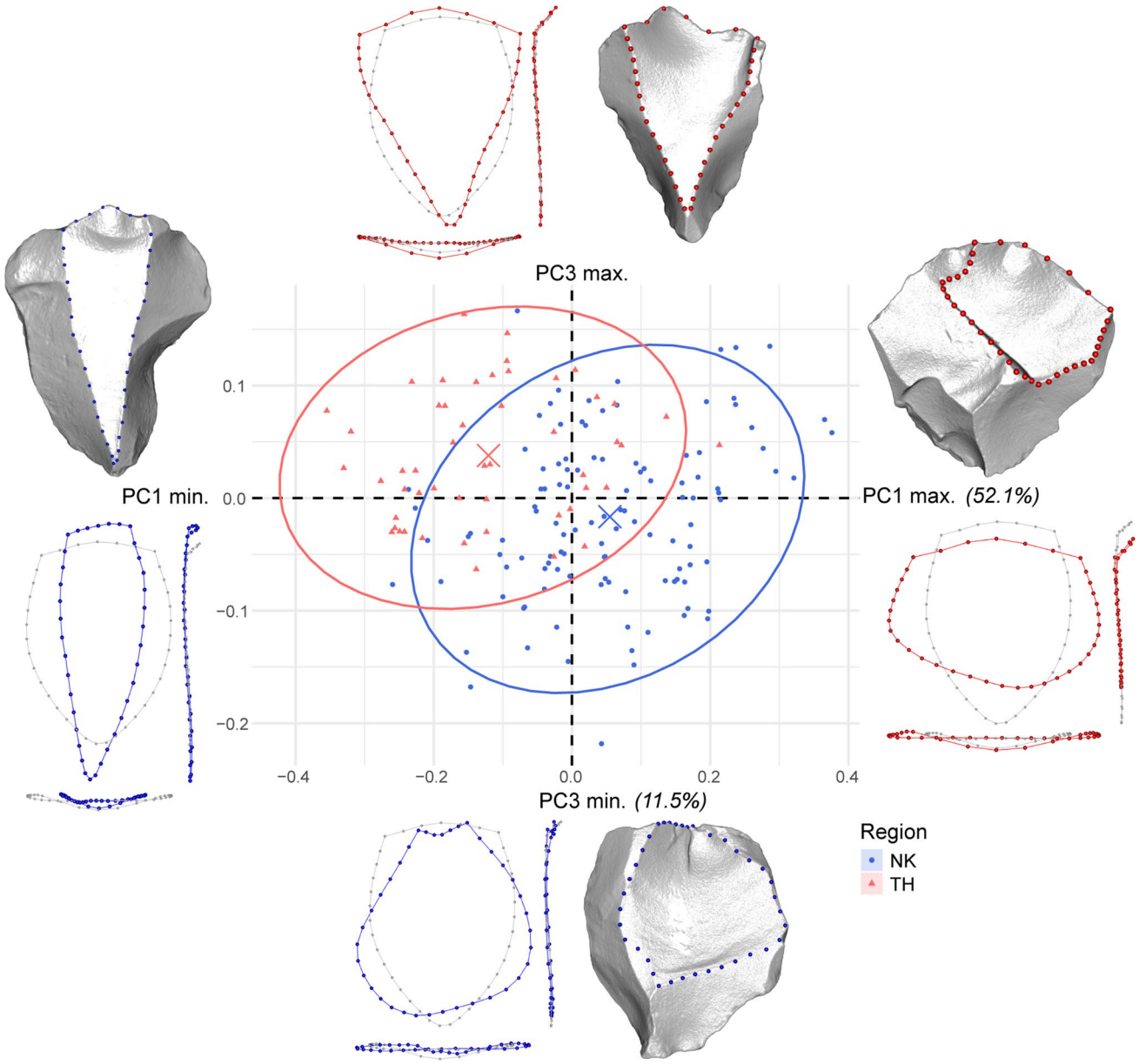

Fig. 5 PCA plot of principal components 1 and 3 for preferential scars, grouped by region. The mean PC score for each group is indicated by a cross (X). Mean (grey), minimum (blue), and maximum (red) theoretical shapes are depicted alongside actual minimum and maximum specimen shapes

identifies strong covariation between core outline and scar shape in general – supporting the expectation of Levallois reduction – the linear regression results suggest that core outline shape alone is not a fully predictive determinant of scar shape. This may be due to the final scars capturing a range of states of core reduction, as well as knapping errors that cause early flake termination, thus not achieving a predetermined shape.

A further test of predetermination in the Levallois reduction process involves measuring the degree of shape standardisation among the samples. Standardisation is calculated as the coefficient of variation (CV) based on the Procrustes distance from the mean shape (Muller and Clarkson 2023). The CV for overall core shape was similarly low for all assemblages with a mean of 21 (range: 20–22, Table S22). For preferential scar shape, there was lower standardisation and more inter-assemblage variability, with the lowest and highest CV values for TH.571 (26) and TH.584 (39), while the NK sites ranged between 31 and 39 (mean: 36). The products from NK have a mean CV of 30 (range: 28–32), suggesting slightly higher standardisation in products at the sites than reflected by core removals. However, this may

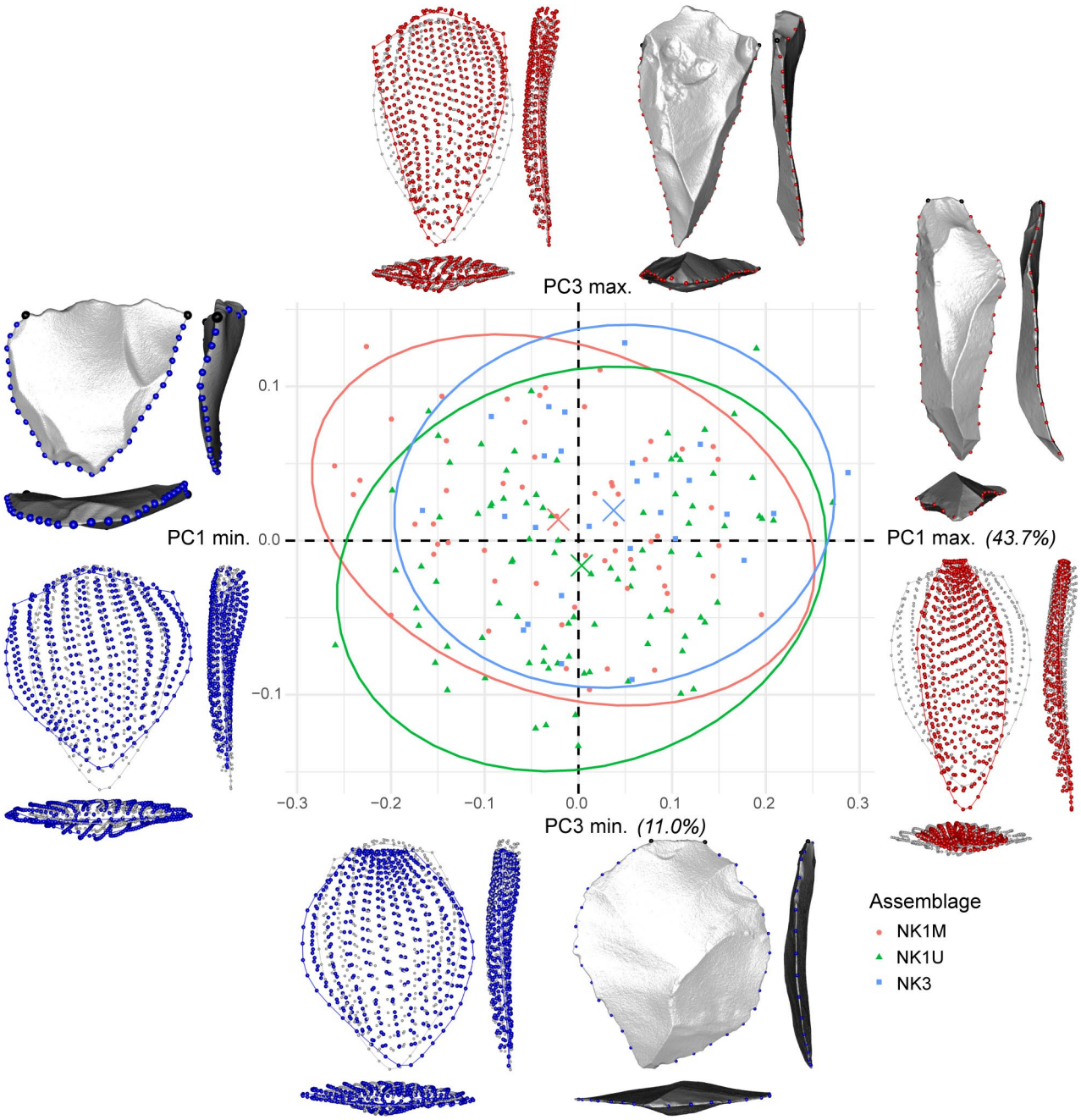

Fig. 6 PCA plot of principal components 1 and 3 for Nazlet Khater end-products grouped by assemblage. The mean PC score for each group is indicated by a cross (X). Mean (grey), minimum (blue), and maximum (red) theoretical shapes are depicted alongside actual minimum and maximum specimen shapes

be influenced by the extent of core reduction, removal of products of certain shapes, or product sample selection which favoured convergent distal morphologies. It has been argued elsewhere that Nubian Levallois is a highly standardised reduction method compared with other Levallois methods (Groucutt and Rose 2023), and Dhofar in particular shows higher levels of size standardisation than Nubian cores from other regions (Samawi and Hallinan 2024). The observed covariance between core and scar shape supports a deliberate relationship in Nubian Levallois reduction, yet less standardisation in end-product shape is observed in each region. Since the final scar shape only represents the last stage of core reduction, it cannot account for the products from earlier phases – a general limitation in lithic studies (Dibble et al. 2017). Despite this, strong similarities between NK products and core scars suggest the final scar is

Table 4 Results of two-block Partial Least Square and linear regression analyses examining covariation between core outline (Block 1/predictor) and preferential scar outline (Block 2/response)

	Two-block partial least square				Linear regression				
Sample	r-PLS	Z	P	% covar	S	R^2	Adjust. R^2	F	P
All	0.629	6.342	0.001 ***	86.6	0.060	0.395	0.391	106.5	0.000 ***
NK	0.463	3.030	0.003 **	57.6	0.062	0.214	0.207	30.5	0.000 ***
TH	0.559	1.295	0.102	57.4	0.057	0.313	0.299	22.3	0.000 ***
Type 1	0.525	3.382	0.001 ***	81.5	0.064	0.276	0.268	34.7	0.000 ***
Type 2	0.718	1.896	0.028 *	69.85	0.049	0.516	0.498	27.7	0.000 ***
Type 1/2	0.595	1.781	0.036 *	81.44	0.060	0.395	0.338	21.9	0.000 ***

r-PLS PLS correlation coefficient; *Z* Effect size; *S* Residual standard error; R^2 Coefficient of determination; *F* Goodall's F-statistic; *P* Significance levels: $P < 0.001$ (***), $P < 0.01$ (**), $P < 0.05$ (*).

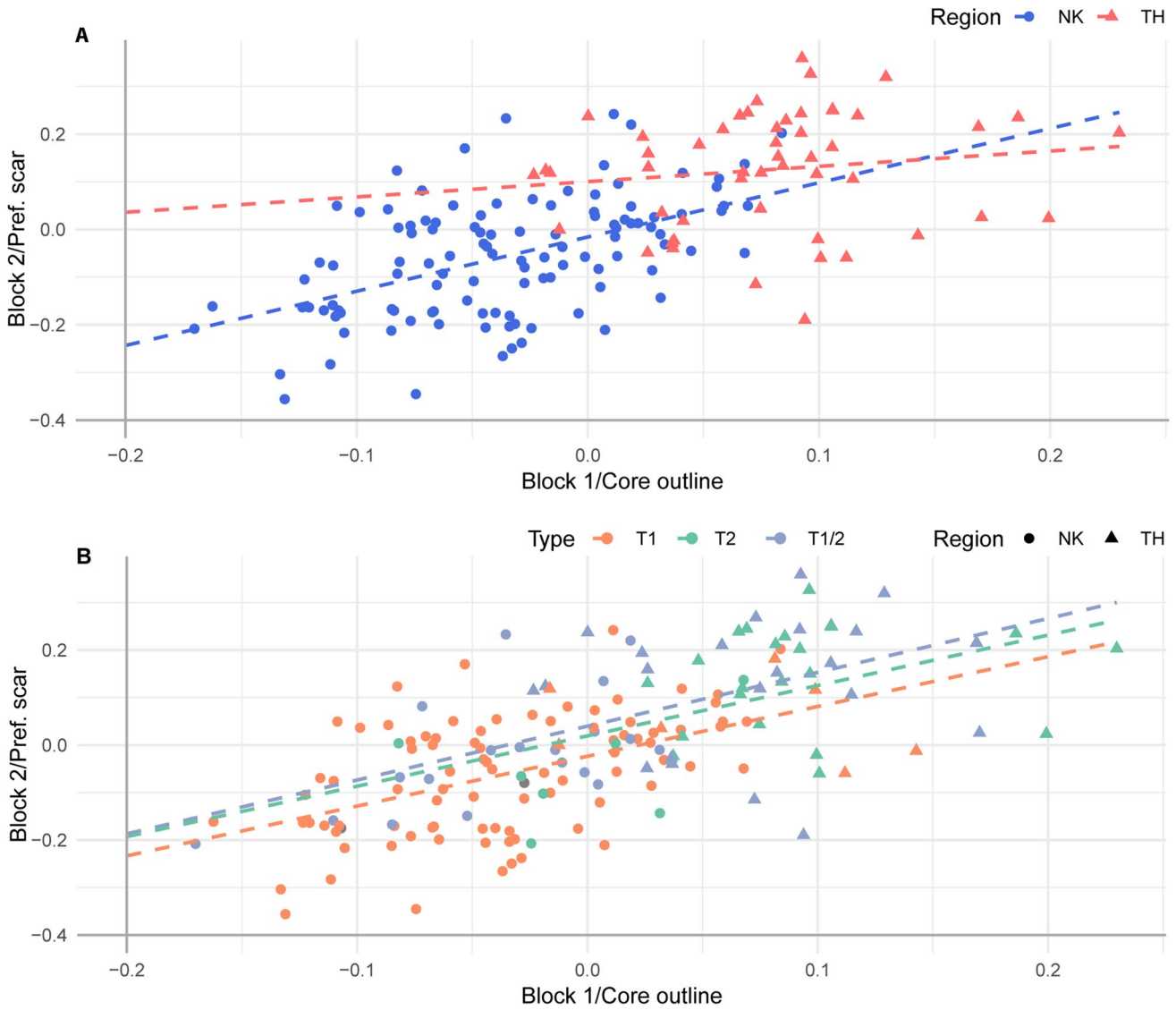

Fig. 7 Linear regression of the first dimension of two-block partial least squares scores for core outline (Block 1) and preferential scar (Block 2). **A** by region, **B** by core type

nevertheless a useful proxy for end-product shape, allowing insights into the goals of Nubian Levallois production even when products are scarce in assemblages.

Discussion

Our analyses present a new replicable protocol for applying GM techniques to Levallois cores to study shape – a key characteristic of the Levallois concept. Using Nubian cores from two regions as a case study, we tested a series of expectations concerning different aspects of shape variability arising out of previous discussions of Levallois technology. The widely accepted definition of Levallois conceptualises the core as two hierarchically-organised surfaces, whose convexities are carefully controlled to produce a specific predetermined product shape (Boëda 1995). Boëda (2013) further introduced the characteristic of "autocorrelation", meaning that the overall shape of Levallois cores is preserved, regardless of size due to progressive reduction. Our results support this by demonstrating low allometry at an intra-assemblage scale, even though there are marked size differences between cores regionally.

Van Peer's (1992) prior refitting and attribute-based study of the NK assemblages found that the organisation of scar ridges (i.e. the preparation strategy) was a stronger determinant of end-product shape than core shape itself. While his work specifically compared Nubian and Classical cores, we tested variation between Nubian reduction strategies. GM analysis showed that the strongest influence of preparation (i.e. core type) was on the relative volume and convexity of the core surfaces, rather than outline shape. Type 1 (distal preparation) cores had a shallower upper surface convexity than Type 2 (bilateral) cores. However, this pattern may be influenced by region since NK cores are predominantly Type 1 whereas TH contributes the most Type 2 cores. Other Nile Valley sites show more variation in the Nubian strategy applied, seeing higher frequencies of Type 2 and 1/2 cores (Olszewski et al. 2010; Samawi and Hallinan 2024). Based on samples from Abydos (90 km from NK), Chiotti et al. (2009) argue for fluidity between Nubian preparation strategies, observing minimal differences in size and shape that, they reason, negate differentiation between core types. Comparisons of these and other assemblages with varying proportions of distal and lateral preparation (e.g. Usik et al. 2013; Oron et al. 2024) may help to further clarify the relative role of region and scar organisation on Nubian core (and end-product) shape.

For Bordes (1950, 1980), differences in Levallois core morphology were fundamentally linked to end-product shape, serving as a key factor in distinguishing between different core types (i.e. Levallois flake, point and blade cores). Our analysis of covariation between scar and core shape confirms that this principle applies to Nubian cores specifically, revealing a strong relationship between the two. Although pointed end-products are often regarded as the primary target of Nubian reduction, GM captures a variety of preferential scar shapes (i.e. ovate to pointed), that correspond with end-product variability at NK. In prior study of the NK assemblages, Van Peer (1992) observed that Nubian end-products were more standardised than those from centripetal Levallois cores, proposing that the Nubian preparation strategy allowed for better shape control. However, Van Peer also noted that distinguishing between Nubian and centripetal end-products was not straightforward, as suggested by the presence of less pointed flake-like scar shapes on NK Nubian cores. In other Nile Valley contexts, the low frequency of pointed end-products has prompted the suggestion that pointedness may not be as critical for Nubian core products as generally assumed (Chiotti et al. 2009). Many studies observe that end-product elongation is a characteristic that differentiates Nubian from other Levallois (point) methods (Van Peer 1992; Usik et al. 2013; Hilbert et al. 2016; Oron et al. 2024; Samawi and Hallinan 2024); therefore, extending GM comparisons to include other Levallois core types could further test the distinctiveness of Nubian end-product shape.

In the only previous GM study of Levallois core morphology, Lycett and von Cramon-Taubadel (2013) predicted that the planform shape of Levallois cores was more likely to reflect spatial or temporal variations than surface topology, citing Nubian cores as one example. Our results show that the aspects of shape represented by PC1 (explaining 20% of variance) and PC2 (15%) do primarily relate to outline shape, specifically in terms of elongation (PC1) and distal skew (PC2). Only elongation showed regionally significant differences, whereby TH cores were more elongated than NK samples. However, PC1 also describes the convexity of the upper surface at its distal end – capturing a defining feature of Nubian cores, the distal median ridge. This also shows clear regional patterns on PC3 (11% of variance) which encompasses differences in relative surface volume and convexity. The Levallois concept defined by Boëda (1995) specifies that Levallois cores must possess hemispheres or surfaces with asymmetric volumes, that serve different, non-interchangeable roles during reduction. While there is a general tendency for the lower surface volume to be greater than the upper surface (e.g. for classic centripetal preferential cores), cores showing the inverse are not necessarily excluded from Levallois if all other criteria are met (maintenance of distal and lateral convexities, prepared striking platforms, exploitation parallel to the plane of intersection). Thus, while NK Nubian cores adhere very closely to this typical distribution of volumes, TH cores tend to show a steep upper (exploitation) surface with greater volume. On many TH specimens, the lower surface has very limited preparation, except for at the distal platform. One explanation for this may be that a naturally tabular shape of the raw

material blocks provided the required ~ 80–90-degree angle for shaping of the upper face, without the need for extensive lower surface removals (Brantingham and Kuhn 2001).

The DMR on a Nubian core serves a critical role in guiding the removal of the preferential product, and therefore in determining its (usually) pointed shape. While Van Peer's (1992) study of the NK cores did not explicitly quantify the ridge angle, the organisation of guiding ridges, their position and inclination were key to his explanation of Levallois shape control and thus the distinction between centripetal and Nubian reduction. In their study of Dhofar assemblages, Usik et al. (2013) introduced measurement of the DMR steepness, grouping angles of less than 60°, 60–90° and 90–120°. They observed most specimens to fall in the steep to semi-steep (< 90°) range – an observation generally supported by the few other studies that measure Nubian core ridge angles (Goder-Goldberger et al. 2016; Hilbert et al 2016; Hallinan and Shaw 2020; Oron et al. 2024). However, the Dhofar assemblages in general have a much higher incidence of steep (< 60°) angles than other regions, such as South Africa (5% of measured ridges), the Negev (28–36%), and central Arabia (24–58%). DMR measurements for new Nubian core collections from the Nile Valley, near Luxor, show a mean angle of 90° (range: 60–110°) (Hallinan, unpublished data). These regional trends of relative distal ridge steepness were captured through GM, on PCs 1 and 3, indicating that Dhofar cores have a generally steeper distal ridge convexity than Nile Valley cores. The application of GM to further assemblages will be an important next step in verifying the range and extent of regional patterns in DMR angle. This approach is particularly valuable given the demonstrated limitations in replicating manual (e.g. goniometer) angle measurements (Dibble and Bernard 1980; Pargeter et al. 2023). In recent (currently unpublished) replication tests between six analysts measuring the DMR on 30 Dhofar Nubian cores, these showed inter-analyst deviation by as much as 40°, with measurements by an analyst on the same specimen on different occasions showing up to 30° differences. While applying digital angle measurement tools to 3D models may, in part, solve the replicability issue, there are still numerous complex and subjective parameters that the user must decide on that introduce potential variability (e.g. the exact measurement point where two surfaces intersect, the measurement radius, the topology of the surfaces being compared, etc.) (Valletta et al. 2020; Yezzi-Woodley et al. 2021; Schunk et al. 2023; Muller et al. 2024). Thus, comparing the overall shape profile of the DMR remains the most reliable way of capturing its steepness over measuring angles at single points.

Nubian cores were a suitable test case for developing our GM protocol because of their clear equivalent morphological features that can be identified across specimens. Similarly, the volumetric structure of other preferential Levallois core forms allows for the landmarking of homologous features, even in the absence of a clear distal point, provided that the orientation is consistent. To test the flexibility of our landmarking methodology on cores without a distal landmark, we re-ran our SLM processing and PCA analyses on the existing sample, treating only the two ends of the proximal platform as fixed landmarks. This modification resulted in a higher failure rate during the deformation of the patched SLM template over the core; seven specimens failed to deform and a further 22 experienced inversions between the patched faces. This indicates that the third (distal) landmark plays an important role in orientation and should be used where possible. Nevertheless, a substantial portion of the dataset using the modified protocol was suitable for GM analysis without requiring further steps to correctly deform the surface patch template (83% of the original specimens), with PCA capturing the same underlying shape structure of the data on the reduced sample, including strong regional differences. To improve success in the data preparation phase, a further step at the landmarking stage can be used to resolve face inversion, through the addition of two temporary landmarks, one on each face positioned at the model centroid (centre of gravity) to ensure consistent placement between specimens. These landmarks ensure that patches are placed on the correct face during deformation, but should be removed prior to Procrustes alignment and further analysis. Therefore, our method can be adapted with high success to other core types, provided that they possess homologous features for alignment. This is particularly important in facilitating future comparisons between Nubian and other Levallois cores to assess the distinctiveness of the Nubian reduction method (cf. Blinkhorn et al. 2021b).

The advantages of 3D GM over traditional metrics in quantifying Levallois core shape have been demonstrated through this study of Nubian core variability. This is particularly evident in the shape characteristics captured by PCs 3, 5 and 6, which relate to convexity and relative surface volume – features that are difficult to represent using standard metrics. While the metric index of flattening indicates that NK cores are generally flatter than TH cores, this clearly oversimplifies the variability in core profile shape. Although GM can identify shape differences, interpreting the behavioural reasons behind them remains complex and this is not fully explored here. Factors related to raw material, technological efficiency, product function, cultural traditions and demographic relationships may all play a role and are important for future model testing (Samawi and Hallinan 2024).

Conclusion

The definition of Levallois technology has shifted from an emphasis on the outline shape of blanks produced (Bordes 1950, 1980), to the geometric configuration of the core as a

three-dimensional volume (Boëda 1988, 1994, 1995). While controlling shape is a fundamental principle, a wide range of core morphologies can fall within classifications of Levallois technology, produced using different reduction strategies (Brantingham and Kuhn 2001). Nubian Levallois is a distinctive method, resulting in cores that possess specific technological and morphological features that have largely been explored through traditional metric, attribute and refitting analyses (e.g. Van Peer 1992; Chiotti et al. 2009; Usik et al. 2013; Hallinan and Shaw 2020; Oron et al. 2024; Samawi and Hallinan 2024). Our study demonstrates that 3D GM is a powerful analytical tool for quantifying shape variation, allowing the identification of nuanced patterning in regional and technological variability. Given current debate over the definition, distinctiveness, and distribution of Nubian cores (Hallinan et al. 2022a, 2022b; Hallinan 2024), forthcoming application of this method to further samples from additional regions will provide important contributions to understanding variability, informing broader patterns of human adaptation and dispersal at an inter-regional scale.

Three-dimensional scanning and methods of analysis are rapidly expanding in lithic research, especially in relation to cores which are fundamentally 3D volumes and inadequately captured by 2D measurements (e.g. Clarkson et al. 2006; Lycett et al. 2010; Shott and Trail 2010; Lycett and von Cramon-Taubadel 2013; Bretzke and Conard 2012; Porter et al. 2019; Ranhorn et al. 2019; Valletta et al. 2021; Grosman et al. 2022; Wyatt-Spratt 2022; Lombao et al. 2023; Lin et al. 2024). The increasing accessibility of 3D modelling technologies (e.g. Porter et al. 2016; Magnani et al. 2020), growing emphasis on replicability (Pargeter et al. 2023), and creating digital archives (e.g. Douglass et al. 2017; Magnani et al. 2018; Di Maida and Hageneuer 2022) has already seen a marked shift in the field of lithic analysis towards GM and other 3D approaches (Wyatt-Spratt 2022). Due to orientation and homology requirements, 3D GM methods will never be applicable to all lithic artefact types and research questions, which limits its uptake in many studies. Additionally, the time invested in 3D scanning and landmarking may be perceived disadvantages of the method compared to traditional attribute recording, but computational advances in automation tools and machine learning offer potential solutions to this in the future (e.g. Barone et al. 2018; Herzlinger and Grosman 2018; Courtenay et al. 2020; González-Molina et al. 2020; Gellis et al. 2022; Grosman et al. 2022).

The importance of open-source methods has been demonstrated by the wide uptake of GM software AGMT3-D in a range of lithic studies (e.g. Herzlinger et al. 2017; Herzlinger and Grosman 2018; Delpiano and Uthmeier 2020; Shipton and White 2020; Hashemi et al. 2021; Li et al. 2021; Falcucci and Peresani 2022; Falcucci et al. 2022; García-Medrano et al. 2020, 2022). However, while AGMT3-D's automatic orientation protocol is suitable for artefacts with certain morphologies, such as handaxes, points, bladelets and backed tools, our tests of its performance on cores, especially Nubian cores, had more limited success. GM analysis often also uses the open platform R, employing packages developed for the biological sciences, such as geomorph and Morpho (e.g. Archer et al. 2015, 2018, 2021; Schoville et al. 2023), with promising potential in development of the Lithics3D package (Pop 2024). Nevertheless, the code, data and methods are rarely shared in full (although see Timbrell et al. 2022a; Hussain et al. 2023; Selden 2023; Thulman et al. 2023 (2D GM); Bustos-Pérez et al. 2024 (3D GM)). The methodology presented here, supported by fully-available R script and data, aims to meet the increasing demand for replicable and reproducible methods in archaeology, particularly lithic studies (e.g. Marwick 2017; Karoune and Plomp 2022; Timbrell et al. 2022b; Araujo et al. 2023; Di Maida et al. 2023; Pargeter et al. 2023), offering a novel application of 3D GM to Levallois technology that can be adapted to other types of cores with highly structured geometries.

Supplementary information The online version contains supplementary material available at https://doi.org/10.1007/s12520-025-02199-2.

Acknowledgements We are grateful to Philip Van Peer (Nazlet Khater) for study permission and facilitating access to the assemblages. The Belgium Middle Egypt Prehistoric Project that excavated the NK sites was directed by Pierre Vermeersch. We also thank Jeffrey Rose, the ARDUQ expedition team, and the Ministry of Heritage and Tourism of the Sultanate of Oman for access to the Dhofar assemblages.

Author contributions E.H. carried out conceptualization, funding acquisition, investigation, methodology and writing of the original draft. J.C. assisted with developing the methodology, and contributed to review and editing.

Funding Open access funding provided by FCT|FCCN (b-on). This research was funded by the European Union Horizon 2020 Framework under the Marie Skłodowska-Curie Grant Agreement No. 891917, awarded to Emily Hallinan, hosted by João Cascalheira (project TANKwA), and by the Fundação para a Ciência e a Tecnologia, I.P. (FCT,https://ror.org/00snfqn58), under Grant 2021/00041.CEECIND/CP1672/CT0007, awarded to Emily Hallinan (project NUBIAN). João Cascalheira is currently funded by the European Union (ERC-CoG-2021, FINISTERRA, 101045506). Views and opinions expressed are however those of the author(s) only and do not necessarily reflect those of the European Union or the European Research Council Executive Agency. Neither the European Union nor the granting authority can be held responsible for them. Fieldwork in Oman was supported by Anthony Marks and the Praemium Academiae of the Czech Academy of Sciences (Viktor Cerny). For the purpose of Open Access, the authors have applied a CC-BY public copyright license to any Author's Accepted Manuscript (AAM) version arising from this submission.

Data availability All data are available in the main text or the supplementary materials. All data, R code and protocols required to replicate the analyses are available in the accompanying research compendium available from the external repository https://doi.org/10.17605/OSF.IO/SJ8ZV.

Declarations

Competing interests The authors declare no competing interests.

References

Adams DC, Rohlf FJ, Slice DE (2004) Geometric morphometrics: ten years of progress following the 'revolution.' Ital J Zool 71:5–16. https://doi.org/10.1080/11250000409356545

Adams DC, Otárola-Castillo E (2013) geomorph: an R package for the collection and analysis of geometric morphometric shape data. Methods Ecol Evol 12:393–399. https://doi.org/10.1111/2041-210X.12035

Adams D, Collyer M, Kaliontzopoulou A, Baken E (2024) Geomorph: Software for geometric morphometric analyses. R package version 4.0.8. https://cran.r-project.org/package=geomorph. Accessed 06/03/2025

Araujo RP, Riede F, Okumura M, Araujo AGM, Leplongeon A, Wren C, Rabuñal JR, Cardillo M, Cruz MB, Matzig DN (2023) Benchmarking methods and data for the whole-outline geometric morphometric analysis of lithic tools. Evol Anthropol 32:124–127. https://doi.org/10.1002/evan.21981

Archer W, Braun DR (2010) Variability in bifacial technology at Elandsfontein, Western Cape, South Africa: a geometric morphometric approach. J Archaeol Sci 37:201–209. https://doi.org/10.1016/j.jas.2009.09.033

Archer W, Gunz P, van Niekerk KL, Henshilwood CS, McPherron SP (2015) Diachronic change within the Still Bay at Blombos Cave, South Africa. PLoS ONE 10(7). https://doi.org/10.1371/journal.pone.0132428

Archer W, Pop CM, Gunz P, McPherron SP (2016) What is still bay? Human biogeography and bifacial point variability. J Hum Evol 97:58–72. https://doi.org/10.1016/j.jhevol.2016.05.007

Archer W, Pop CM, Rezek Z, Schlager S, Lin SC, Weiss M, Dogandžić T, Desta D, McPherron SP (2018) A geometric morphometric relationship predicts stone flake shape and size variability. Archaeol Anthropol Sci 10:1991–2003. https://doi.org/10.1007/s12520-017-0517-2

Archer W, Presnyakova D (2019) Considerations in the application of 3DGM to stone artifacts with a focus on orientation error in bifaces. In: Seguchi N, Dudzik B (eds) 3D data acquisition for bioarchaeology, forensic anthropology, and archaeology. Academic Press, pp 161–173. https://doi.org/10.1016/b978-0-12-815309-3.00008-5

Archer W, Djakovic I, Brenet M, Bourguignon L, Presnyakova D, Schlager S, Soressi M, McPherron SP (2021) Quantifying differences in hominin flaking technologies with 3D shape analysis. J Hum Evol 150. https://doi.org/10.1016/j.jhevol.2020.102912

Baken E, Collyer M, Kaliontzopoulou A, Adams D (2021) geomorph v4.0 and gmShiny: enhanced analytics and a new graphical interface for a comprehensive morphometric experience. Methods Ecol Evol 12:2355–2363. https://doi.org/10.1111/2041-210X.13723

Bar-Yosef O, Dibble H (1995) Preface. In: Dibble HL, Bar-Yosef O (eds) The definition and interpretation of Levallois variability. Prehistory Press

Barone S, Neri P, Paoli A, Razionale AV (2018) Automated technical documentation of lithic artefacts by digital techniques. Digit Appl Archaeol Cult Herit 11. https://doi.org/10.1016/j.daach.2018.e00087

Blinkhorn J, Groucutt HS, Scerri EML, Petraglia MD, Blockley S (2021) Directional changes in Levallois core technologies between Eastern Africa, Arabia, and the Levant during MIS 5. Sci Rep 11:11465. https://doi.org/10.1038/s41598-021-90744-z

Blinkhorn J, Zanolli C, Compton T, Groucutt HS, Scerri EML, Crété L, Stringer C, Petraglia MD, Blockley S (2021) Nubian Levallois technology associated with southernmost Neanderthals. Sci Rep 11:2869. https://doi.org/10.1038/s41598-021-82257-6

Bookstein FL (1991) Morphometric tools for landmark data: geometry and biology. Cambridge University Press, Cambridge

Boëda E (1988) Le concept Levallois et évaluation de son champ d'application. In: Otte M (ed) L'Homme de Néandertal, Vol. 4: La technique. University of Liège 13–26.

Boëda E (1994) Le concept Levallois: Variabilité des méthodes. CNRS Editions, Paris

Boëda E (1995) Levallois: a volumetric construction, methods, a technique. In: Dibble HL, Bar-Yosef O (eds) The definition and interpretation of Levallois variability. Prehistory Press 41–69.

Boëda E (2013) Techno-logique & Technologie: Une paléo-histoire des objets lithiques tranchants. @rchéo-éditions

Bordes F (1950) Principes d'une méthode d'étude des techniques de débitage et de la typologie du Paléolithique ancien et moyen. L'anthropol 54:19–34

Bordes F (1961) Typologie du Paléolithique ancien et moyen. Publications de l'Institut de Préhistoire de l'Université de Bordeaux

Bordes F (1980) Le débitage Levallois et ses variantes. Bull Soc Préhist Fr 77:45–49. https://doi.org/10.3406/bspf.1980.5242

Boucher de Perthes J (1857) Antiquités celtiques et antédiluviennes: Mémoire sur l'industrie primitive et les arts à leur origine. Treuttel et Wurtz, Paris

Brantingham PJ, Kuhn SL (2001) Constraints on Levallois core technology: a mathematical model. J Archaeol Sci 28:747–761. https://doi.org/10.1006/jasc.2000.0594

Bretzke K, Conard N (2012) Evaluating morphological variability in lithic assemblages using 3D models of stone artifacts. J Archaeol Sci 39:3741–3749. https://doi.org/10.1016/j.jas.2012.06.039

Buchanan B, Hamilton MJ, Macdonald D, Blinkhorn J, Groucutt HS, Eren MI, Kuhn SL (2023) Geometric morphometric analyses of Levallois points from the Levantine Middle Paleolithic do not support functional specialization. Lithic Technol 48(4):437–451. https://doi.org/10.1080/01977261.2023.2208930

Bustos-Pérez G, Gravina B, Brenet M, Romagnoli F (2024) The contribution of 2D and 3D geometric morphometrics to lithic taxonomies: testing discrete categories of backed flakes from recurrent centripetal core reduction. J Paleolithic Archaeol 7(5). https://doi.org/10.1007/s41982-023-00167-7

Chacón MG, Détroit F, Coudenneau A, Moncel M-H (2016) Morphometric assessment of convergent tool technology and function during the Early Middle Palaeolithic: the case of Payre, France. PLoS ONE 11(5). https://doi.org/10.1371/journal.pone.0155316

Chiotti L, Dibble HL, Olszewski DI, McPherron SP, Schurmans UA (2009) Middle Palaeolithic lithic technology from the Western

High Desert of Egypt. J Field Archaeol 34:307–318. https://doi.org/10.1179/009346909791070862
Clarkson C, Vinicius L, Lahr MM (2006) Quantifying flake scar patterning on cores using 3D recording techniques. J Archaeol Sci 33:132–142. https://doi.org/10.1016/j.jas.2005.07.007
Commont V (1909) L'industrie mousterienne dans le Nord de la France. In: Congrès Préhistorique de France, 5ème session, Paris, pp 115–157
Copeland L (1983) Levallois/non-Levallois determinations in the early Levant Mousterian: problems and questions for 1983. Paléorient 9:15–27. https://doi.org/10.3406/paleo.1983.4338
Courtenay LA, Huguet R, González-Aguilera D, Yravedra J (2020) A hybrid geometric morphometric deep learning approach for cut and trampling mark classification. Appl Sci 10(1):150. https://doi.org/10.3390/app10010150
de Mortillet G (1883) Le Préhistorique, antiquité de l'Homme. Reinwald, Paris
Delpiano D, Uthmeier T (2020) Techno-functional and 3D shape analysis applied for investigating the variability of backed tools in the Late Middle Paleolithic of Central Europe. PLoS ONE 15. https://doi.org/10.1371/journal.pone.0236548
Delpiano D, Gennai J, Peresani M (2021) Techno-functional implication on the production of discoid and Levallois backed implements. Lithic Technol 46(3):171–191. https://doi.org/10.1080/01977261.2021.1886487
Di Maida G, Hageneuer S (2022) The DISAPALE project: a new digital repository of lithic and bone artefacts. Lithic Technol 47(4):283–295. https://doi.org/10.1080/01977261.2022.2048511
Di Maida G, Hattermann M, Delpiano D (2023) 3D models of lithic artefacts: a test on their efficacy. Digital Appl Archaeol Cult Heritage 30. https://doi.org/10.1016/j.daach.2023.e00279
Dibble HL, Bernard MC (1980) A comparative study of basic edge angle measurement techniques. Am Antiquity 45:857–865. https://doi.org/10.2307/280156
Dibble HL, Bar-Yosef O (eds) (1995) The definition and interpretation of Levallois variability. Prehistory Press, Madison, Wisconsin
Dibble HL, Holdaway SJ, Lin SC, Braun DR, Douglass MJ, Iovitá R, McPherron SP, Olszewski DI, Sandgathe D (2017) Major fallacies surrounding stone artifacts and assemblages. J Archaeol Method Theory 24:813–851. https://doi.org/10.1007/s10816-016-9297-8
Douglass M, Kuhnel D, Magnani M, Hittner L, Chodoronek M, Porter S (2017) Community outreach, digital heritage and private collections: a case study from the North American Great Plains. World Archaeol 49(5):623–638. https://doi.org/10.1080/00438243.2017.1309299
Eerkens JW, Bettinger RL (2001) Techniques for assessing standardization in artifact assemblages: can we scale material variability? Am Antiquity 66:493–504. https://doi.org/10.2307/2694247
Eren MI, Lycett SJ (2016) A statistical examination of flake edge angles produced during experimental lineal Levallois reductions and consideration of their functional implications. J Archaeol Method Theory 23:379–398. https://doi.org/10.1007/s10816-015-9245-z
Eren MI, Lycett SJ (2012) Why Levallois? A morphometric comparison of experimental "preferential" Levallois flakes versus debitage flakes. PLoS ONE 7(1). https://doi.org/10.1371/journal.pone.0029273
Falcucci A, Peresani M (2022) The contribution of integrated 3D model analysis to Protoaurignacian stone tool design. PLoS ONE 17. https://doi.org/10.1371/journal.pone.0268539
Falcucci A, Karakostis FA, Goeldner D, Peresani M (2022) Bringing shape into focus: assessing differences between blades and bladelets and their technological significance in 3D form. J Archaeol Sci Rep 43. https://doi.org/10.1016/j.jasrep.2022.103490
Foley RA, Lahr MM (1997) Mode 3 technologies and the evolution of modern humans. Camb Archaeol J 7:3–36. https://doi.org/10.1017/s0959774300001451
García-Medrano P, Maldonado-Garrido E, Ashton N, Ollé A (2020) Objectifying processes: the use of geometric morphometrics and multivariate analyses on Acheulean tools. J Lithic Stud 7(1). https://doi.org/10.2218/jls.4327
García-Medrano P, Shipton C, White M, Ashton N (2022) Acheulean diversity in Britain (MIS 15-MIS 11): from the standardization to the regionalization of technology. Front Earth Sci 10. https://doi.org/10.3389/feart.2022.917207
Gellis J, Rangel Smith C, Foley RA (2022) PyLithics: A Python package for stone tool analysis. J Open Source Softw 7(69):3738. https://doi.org/10.21105/joss.03738
González-Molina I, Jiménez-García B, Maíllo-Fernández JM, Baquedano E, Domínguez-Rodrigo M (2020) Distinguishing discoid and centripetal Levallois methods through machine learning. PLoS ONE 15(12). https://doi.org/10.1371/journal.pone.0244288
Goodall C (1991) Procrustes methods in the statistical analysis of shape. J R Stat Soc Ser B (Methodological) 53(2):285–321. https://doi.org/10.1111/j.2517-6161.1991.tb01825.x
Goder-Goldberger M, Gubenko N, Hovers E (2016) "Diffusion with modifications": Nubian assemblages in the central Negev highlands of Israel and their implications for Middle Paleolithic interregional interactions. Quat Int 408:121–139. https://doi.org/10.1016/j.quaint.2016.02.008
Guichard J, Guichard G (1965) The early and middle palaeolithic of Nubia: preliminary results. In: Wendorf F (ed) Contributions to the prehistory of Nubia. South Methodist Univ Press 57–116
Grosman L, Muller A, Dag I, Goldgeier H, Harush O, Herzlinger G, Nebenhaus K, Valetta F, Yashuv T, Dick N (2022) Artifact3-D: new software for accurate, objective and efficient 3D analysis and documentation of archaeological artifacts. PLoS ONE 17. https://doi.org/10.1371/journal.pone.0268401
Groucutt HS, Rose JI (2023) Standardization of Nubian Levallois technology in Dhofar, southern Arabia. Lithic Technol 48:422–436. https://doi.org/10.1080/01977261.2023.2211878
Hallinan E, Shaw M (2020) Nubian Levallois reduction strategies in the Tankwa Karoo, South Africa. PLoS ONE 15. https://doi.org/10.1371/journal.pone.0241068
Hallinan E, Barzilai O, Bicho N, Cascalheira J, Demidenko Y, Goder-Goldberger M, Hovers E, Marks A, Oron M, Rose J (2022) No direct evidence for the presence of Nubian Levallois technology and its association with Neanderthals at Shukbah Cave. Sci Rep 12:1204. https://doi.org/10.1038/s41598-022-05072-7
Hallinan E, Barzilai O, Beshkani A, Cascalheira J, Demidenko Y, Goder-Goldberger M, Hilbert YH, Hovers E, Marks AE, Nymark A, Olszewski DI, Oron M, Rose J, Shaw M, Usik VI (2022) The nature of Nubian: developing current global perspectives on Nubian Levallois technology and the Nubian Complex. Evol Anthropol 31:227–232. https://doi.org/10.1002/evan.21958
Hallinan E, Marks AE (2023) The complex taxonomy of 'Nubian' in context. J Paleolithic Archaeol 6:23. https://doi.org/10.1007/s41982-023-00151-1
Hallinan E (2024) A synthesis and critical inventory of Nubian cores in Middle Stone Age and Middle Palaeolithic assemblages. J Open Archaeol Data 12(9):1–14. https://doi.org/10.5334/joad.129
Hashemi SM, Nasab HV, Berillon G, Oryat M (2021) An investigation of the flake-based lithic tool morphology using 3D geometric morphometrics: a case study from the Mirak Paleolithic site. Iran J Archaeol Sci Rep 37. https://doi.org/10.1016/j.jasrep.2021.102948
Herzlinger G, Goren-Inbar N, Grosman L (2017) A new method for 3D geometric morphometric shape analysis: the case study of handaxe knapping skill. J Archaeol Sci Rep 14:163–173. https://doi.org/10.1016/j.jasrep.2017.05.013
Herzlinger G, Grosman L (2018) AGMT3-D: a software for 3-D landmarks-based geometric morphometric shape analysis of archaeological artifacts. PLoS ONE 13(11). https://doi.org/10.1371/journal.pone.0207890

Hilbert YH, Crassard R, Rose JI, Geiling JM, Usik VI (2016) Technological homogeneity within the Arabian Nubian Complex: comparing chert and quartzite assemblages from central and southern Arabia. J Lithic Stud 3(2):411–437. https://doi.org/10.2218/jls.v3i2.1420

Hu Y, Marwick B, Zhang JF, Rui X, Hou YM, Yue JP, Chen WR, Huang WW, Li B (2019) Late Middle Pleistocene Levallois stone-tool technology in southwest China. Nature 565:82–85. https://doi.org/10.1038/s41586-018-0710-1

Hu Y, Marwick B, Zhang JF, Rui X, Hou YM, Chen WR, Huang WW, Li B (2019) Robust technological readings identify integrated structures typical of the Levallois concept in Guanyindong Cave, South China. Nat Sci Rev 6:1096–1099. https://doi.org/10.1093/nsr/nwz192

Hublin JJ (2009) The origin of Neandertals. Proc Natl Acad Sci 106:16022–16027. https://doi.org/10.1073/pnas.090411910

Hussain ST, Riede F, Matzig D, Biard M, Crombé P et al (2023) A pan-European dataset revealing variability in lithic technology, toolkits, and artefact shapes ~15-11 kya. Sci Data 10:593. https://doi.org/10.1038/s41597-023-02500-9

Iovita R (2011) Shape variation in Aterian tanged tools and the origins of projectile technology: a morphometric perspective on stone tool function. PLoS ONE 6(12). https://doi.org/10.1371/journal.pone.0029029

Karoune E, Plomp E (2022) Removing barriers to reproducible research in archaeology. Zenodo, ver. 5, peer reviewed and recommended by Peer Community in Archaeology. https://doi.org/10.5281/ZENODO.6615276

Klingenberg CP (2016) Size, shape, and form: concepts of allometry in geometric morphometrics. Dev Genes Evol 226:113–137. https://doi.org/10.1007/s00427-016-0539-2

Lahr MM, Foley RA (2001) Mode 3, *Homo helmei*, and the pattern of human evolution in the Middle Pleistocene. In: Brown KAR (ed) Barham L. Africa and Asia in the Middle Pleistocene. West Acad Specialist Press, Hum Roots 23–39.

Li H, Lei L, Li D, Lotter MG, Kuman K (2021) Characterizing the shape of large cutting tools from the Baise Basin (South China) using a 3D geometric morphometric approach. J Archaeol Sci Rep 36. https://doi.org/10.1016/j.jasrep.2021.102820

Li Y, Boëda E, Forestier H, Zhou Y (2019) Lithic technology, typology and cross-regional comparison of Pleistocene lithic industries: comment on the earliest evidence of Levallois in East Asia. L'anthropologie 123. https://doi.org/10.1016/j.anthro.2019.102728

Lin SC, Clarkson C, Julianto IMA, Ferdianto A, Sutikna T (2024) A new method for quantifying flake scar organisation on cores using orientation statistics. J Archaeol Sci 167. https://doi.org/10.1016/j.jas.2024.105998

Lombao D, Falcucci A, Moos E, Peresani M (2023) Unravelling technological behaviors through core reduction intensity. The case of the early Protoaurignacian assemblage from Fumane Cave. J Archaeol Sci 160. https://doi.org/10.1016/j.jas.2023.105889

Lycett SJ, Cramon-Taubadel NV, Foley RA (2006) A crossbeam coordinate caliper for the morphometric analysis of lithic nuclei: a description, test and empirical examples of application. J Archaeol Sci 33:847–861. https://doi.org/10.1016/j.jas.2005.10.014

Lycett SJ, Cramon-Taubadel NV, Gowlett JA (2010) A comparative 3D geometric morphometric analysis of Victoria West cores: implications for the origins of Levallois technology. J Archaeol Sci 37:1110–1117. https://doi.org/10.1016/j.jas.2009.12.011

Lycett SJ, Eren MI (2013) Levallois economics: an examination of "waste" production in experimentally produced Levallois reduction sequences. J Archaeol Sci 40:2384–2392. https://doi.org/10.1016/j.jas.2013.01.016

Lycett SJ, von Cramon-Taubadel N (2013) A 3D morphometric analysis of surface geometry in Levallois cores: patterns of stability and variability across regions and their implications. J Archaeol Sci 40:1508–1517. https://doi.org/10.1016/j.jas.2012.11.005

Lycett SJ, von Cramon-Taubadel N, Eren MI (2016) Levallois: potential implications for learning and cultural transmission capacities. Lithic Technol 41(1):9–38. https://doi.org/10.1179/2051618515y.0000000012

Magnani M, Guttorm A, Magnani N (2018) Three-dimensional, community-based heritage management of indigenous museum collections: archaeological ethnography, revitalization and repatriation at the Sámi Museum Siida. J Cult Herit 31:162–169. https://doi.org/10.1016/j.culher.2017.12.001

Magnani M, Douglass M, Schroder W, Reeves J, Braun DR (2020) The digital revolution to come: photogrammetry in archaeological practice. Am Antiquity 85(4):737–760. https://doi.org/10.1017/aaq.2020.59

Marwick B (2017) Computational reproducibility in archaeological research: basic principles and a case study of their implementation. J Archaeol Method Theory 24:424–450. https://doi.org/10.1007/s10816-015-9272-9

Muller A, Clarkson C (2023) Filling in the blanks: standardization of lithic flake production throughout the Stone Age. Lithic Technol 48(3):222–236. https://doi.org/10.1080/01977261.2022.2103290

Muller A, Sharon G, Grosman L (2024) Automatic analysis of the continuous edges of stone tools reveals fundamental handaxe variability. Sci Rep 14:7422. https://doi.org/10.1038/s41598-024-57450-y

Okumura M, Araujo AGM (2019) Archaeology, biology, and borrowing: a critical examination of geometric morphometrics in archaeology. J Archaeol Sci 101:149–158. https://doi.org/10.1016/j.jas.2017.09.015

Olszewski DI, Dibble HL, McPherron SP, Schurmans UA, Chiotti L, Smith JR (2010) Nubian Complex strategies in the Egyptian high desert. J Hum Evol 59:188–201. https://doi.org/10.1016/j.jhevol.2010.06.001

Oron M, Hovers E, Porat N, Roskin J, Abulafia T (2024) Nubian Levallois technology during MIS 5: refitted lithic sequences and OSL Ages of Dimona South, Israel, and their broader implications. J Paleolithic Archaeol 7:4. https://doi.org/10.1007/s41982-024-00170-6

Pallo MC (2022) Levallois technology in southern Patagonia (Argentina and Chile): current knowledge and future perspectives. J Lithic Stud 9(1). https://doi.org/10.2218/jls.6449

Pargeter J, Brooks A, Douze K, Eren M, Groucutt HS, McNeil J, Mackay A, Ranhorn K, Scerri E, Shaw M, Tryon C, Will M, Leplongeon A (2023) Replicability in lithic analysis. Am Antiquity 88(2):163–186. https://doi.org/10.1017/aaq.2023.4

Picin A, Vaquero M, Weniger GC, Carbonell E (2014) Flake morphologies and patterns of core configuration at the Abric Romaní rockshelter: a geometric morphometric approach. Quat Int 350:84–93. https://doi.org/10.1016/j.quaint.2014.05.004

Pop C (2024) Lithics3D: A toolbox for 3D analysis of archaeological lithics. R package version 0.5.2, commit c5462ff6a00dbea2f46b63480f9703fac33e3901. https://github.com/cornelmpop/Lithics3D. Accessed 06/03/2025

Porter ST, Roussel M, Soressi M (2016) A simple photogrammetry rig for the reliable creation of 3D artifact models in the field. Lithic examples from the Early Upper Paleolithic sequence of Les Cottés (France). Adv Archaeol Pract 4:71–86. https://doi.org/10.7183/2326-3768.4.1.71

Porter ST, Roussel M, Soressi M (2019) A comparison of Châtelperronian and Protoaurignacian core technology using data derived from 3D models. J Comput Appl Archaeol 2:41–55. https://doi.org/10.5334/jcaa.17

R Core Team (2024) R: A language and environment for statistical computing. R Foundation for Statistical Computing, Vienna, Austria. https://www.R-project.org. Accessed 06/03/2025

Ranhorn KL, Braun DR, Gürbüz REB, Greiner E, Wawrzyniak D, Brooks AS (2019) Evaluating prepared core assemblages with three-dimensional methods: a case study from the Middle Paleolithic at Skhūl (Israel). Archaeol Anthropol Sci 11:3225–3238. https://doi.org/10.1007/s12520-018-0746-z

Rohlf FJ, Corti M (2000) Use of two-block partial least-squares to study covariation in shape. Syst Biol 49(4):740–753. https://doi.org/10.1080/106351500750049806

Rohlf FJ, Marcus LF (1993) A revolution in morphometrics. Trends Ecol Evol 8:129–132. https://doi.org/10.1016/0169-5347(93)90024-j

Rose JI, Usik VI, Marks AE, Hilbert YH, Galletti CS, Parton A, Geiling JM, Černý V, Morley MW, Roberts RG (2011) The nubian complex of Dhofar, Oman: an African Middle Stone Age industry in southern Arabia. PLoS ONE 6(11). https://doi.org/10.1371/journal.pone.0028239

Rose JI, Hilbert YH, Marks AE, Usik VI (2018) The first peoples of Oman: Palaeolithic archaeology on the Nejd Plateau. Ministry of Heritage and Culture, Sultanate of Oman

Rose JI, Usik VI, Hilbert Y, Garba R, Beshkani A, Chlachula D, Jaboob MM, Marks AE (2023) Prehistoric settlement patterns in southern Oman from the Lower Palaeolithic to the Neolithic. Paléorient 49(1):83–108. https://doi.org/10.4000/paleorient.2774

Samawi O, Hallinan E (2024) More than surface finds: Nubian Levallois core metric variability and site distribution across Africa and Southwest Asia. J Paleolithic Archaeol 7(26). https://doi.org/10.1007/s41982-024-00192-0

Sandgathe DM (2004) An alternative interpretation of the Levallois reduction technique. Lithic Technol 29(2):147–159. https://doi.org/10.1080/01977261.2004.11721017

Schlanger N (1996) Understanding Levallois: lithic technology and cognitive archaeology. Camb Archaeol J 6:231–254. https://doi.org/10.1017/s0959774300001724

Schlager S (2017) Morpho and Rvcg – shape analysis in R. In: Zheng G, Li S, Szekely G (eds) Statistical Shape and Deformation Analysis. Academic Press, pp 217–256. https://doi.org/10.1016/b978-0-12-810493-4.00011-0

Schoville BJ, Chiwara-Maenzanise P, Otárola-Castillo E, Wilkins J (2023) Function, style, and standardization: is the proximal or distal end of a Middle Stone Age point more variable? Lithic Technol 48:393–407. https://doi.org/10.1080/01977261.2023.2233167

Schunk L, Cramer A, Bob K, Calandra I, Heinz G, Jöris O, Marreiros J (2023) Enhancing lithic analysis: introducing 3D-EdgeAngle as a semi-automated 3D digital method to systematically quantify stone tool edge angle and design. PLoS ONE 18. https://doi.org/10.1371/journal.pone.0295081

Selden RZ (2023) Morphologically similar, but regionally distinct: Perdiz arrow points from Caddo burial contexts in the American southeast. Lithic Technol 48:62–73. https://doi.org/10.1080/01977261.2022.2095492

Shimelmitz R, Kuhn SL (2018) The toolkit in the core: there is more to Levallois production than predetermination. Quaternary Int 464:81–91. https://doi.org/10.1016/j.quaint.2017.08.011

Shipton C, White M (2020) Handaxe types, colonization waves, and social norms in the British Acheulean. J Archaeol Sci: Rep 31. https://doi.org/10.1016/j.jasrep.2020.102352

Shott MJ, Trail BW (2010) Exploring new approaches to lithic analysis: laser scanning and geometric morphometrics. Lithic Technol 35:195–220. https://doi.org/10.1080/01977261.2010.11721090

Sisk ML, Shea JJ (2009) Experimental use and quantitative performance analysis of triangular flakes (Levallois points) used as arrowheads. J Archaeol Sci 36:2039–2047. https://doi.org/10.1016/j.jas.2009.05.023

Slice DE (2007) Geometric morphometrics. Annu Rev Anthropol 36:261–281. https://doi.org/10.1146/annurev.anthro.34.081804.120613

Timbrell L, de la Peña P, Way A, Hoggard C, Backwell L, d'Errico F, Wadley L, Grove M (2022) Technological and geometric morphometric analysis of 'post-Howiesons Poort points' from Border Cave, KwaZulu-Natal. S Afr Quat Sci Rev 297:107813. https://doi.org/10.1016/j.quascirev.2022.107813

Timbrell L, Scott C, Habte B, Tefera Y, Monod H, Qazzih M, Marais B, Black W, Maroma C, Ndiema E, Henderson S, Elmes K, Plomp K, Grove M (2022) Testing inter-observer error under a collaborative research framework for studying lithic shape variability. Archaeol Anthropol Sci 14:209. https://doi.org/10.1007/s12520-022-01676-2

Thulman DK, Shott MJ, Slade AM, Williams JP (2023) Clovis point allometry, modularity, and integration: exploring shape variation due to tool use with landmark-based geometric morphometrics. PLoS ONE 18. https://doi.org/10.1371/journal.pone.0289489

Tryon CA, McBrearty S, Texier PJ (2005) Levallois lithic technology from the Kapthurin Formation, Kenya: Acheulian origin and Middle Stone Age diversity. Afr Archaeol Rev 22:199–229. https://doi.org/10.1007/s10437-006-9002-5

Usik VI, Rose JI, Hilbert YH, Peer PV, Marks AE (2013) Nubian Complex reduction strategies in Dhofar, southern Oman. Quat Int 300:244–266. https://doi.org/10.1016/j.quaint.2012.08.2111

Van Peer P (1992) The Levallois reduction strategy. Prehistory Press, Madison, Wisconsin

Valletta F, Smilansky U, Goring-Morris AN, Grosman L (2020) On measuring the mean edge angle of lithic tools based on 3-D models–a case study from the southern Levantine Epipalaeolithic. Archaeol Anthropol Sci 12:49. https://doi.org/10.1007/s12520-019-00954-w

Valletta F, Dag I, Grosman L (2021) Identifying local learning communities during the Terminal Palaeolithic in the southern Levant: multi-scale 3-D analysis of flint cores. J Comput Appl Archaeol 4:145–168. https://doi.org/10.5334/jcaa.74

Vermeersch PM, Paulissen E, Gijselings G (1977) Prospection préhistorique entre Asyut et Nag'Hammadi (Egypte). Bull Soc Roy Belge Anthropol Préhist 88:117–124

Vermeersch PM, Paulissen E, Otte M, Gijselings G, Drappier D (1979) Prehistoric and geomorphologic research in Middle Egypt. Palaeoecol Afr Surround Islands 12:111–115

Vermeersch PM, Van Peer P, Paulissen E (2002a) Middle Palaeolithic chert quarrying at Nazlet Khater 1. In: Vermeersch PM (ed) Palaeolithic chert quarrying sites in Upper and Middle Egypt. Leuven Univ Press Leuven 27–78

Vermeersch PM, Van Peer P, Paulissen E (2002b) Middle Palaeolithic chert quarrying at Nazlet Khater 3. In: Vermeersch PM (ed) Palaeolithic quarrying sites in Upper and Middle Egypt. Leuven Univ Press 99–112

Wyatt-Spratt S (2022) After the revolution: a review of 3D modelling as a tool for stone artefact analysis. J Comput Appl Archaeol 5:215–237. https://doi.org/10.5334/jcaa.103

Wynn T, Coolidge FL (2004) The expert Neandertal mind. J Hum Evol 46:467–487. https://doi.org/10.1016/j.jhevol.2004.01.005

Yezzi-Woodley K, Calder J, Olver PJ, Cody P, Huffstutler T, Terwilliger A, Melton JA, Tappen M, Coil R, Tostevin G (2021) The virtual goniometer: demonstrating a new method for measuring angles on archaeological materials using fragmentary bone. Archaeol Anthropol Sci 13:106. https://doi.org/10.1007/s12520-021-01335-y